MALARIA

Mapping functional humoral correlates of protection against malaria challenge following RTS,S/AS01 vaccination

Todd J. Suscovich[1]*†, Jonathan K. Fallon[1]*, Jishnu Das[1]*‡, Allison R. Demas[1,2]*, Jonathan Crain[1], Caitlyn H. Linde[1†], Ashlin Michell[1], Harini Natarajan[3], Claudia Arevalo[1], Thomas Broge[1†], Thomas Linnekin[1†], Viraj Kulkarni[1], Richard Lu[1], Matthew D. Slein[1], Corinne Luedemann[1], Meghan Marquette[2], Sandra March[2], Joshua Weiner[3], Scott Gregory[4], Margherita Coccia[5], Yevel Flores-Garcia[6], Fidel Zavala[6], Margaret E. Ackerman[3], Elke Bergmann-Leitner[7], Jenny Hendriks[8], Jerald Sadoff[8], Sheetij Dutta[7], Sangeeta N. Bhatia[2,9,10,11,12], Douglas A. Lauffenburger[9,13], Erik Jongert[5§], Ulrike Wille-Reece[4§], Galit Alter[1§]

Vaccine development has the potential to be accelerated by coupling tools such as systems immunology analyses and controlled human infection models to define the protective efficacy of prospective immunogens without expensive and slow phase 2b/3 vaccine studies. Among human challenge models, controlled human malaria infection trials have long been used to evaluate candidate vaccines, and RTS,S/AS01 is the most advanced malaria vaccine candidate, reproducibly demonstrating 40 to 80% protection in human challenge studies in malaria-naïve individuals. Although antibodies are critical for protection after RTS,S/AS01 vaccination, antibody concentrations are inconsistently associated with protection across studies, and the precise mechanism(s) by which vaccine-induced antibodies provide protection remains enigmatic. Using a comprehensive systems serological profiling platform, the humoral correlates of protection against malaria were identified and validated across multiple challenge studies. Rather than antibody concentration, qualitative functional humoral features robustly predicted protection from infection across vaccine regimens. Despite the functional diversity of vaccine-induced immune responses across additional RTS,S/AS01 vaccine studies, the same antibody features, antibody-mediated phagocytosis and engagement of Fc gamma receptor 3A (FCGR3A), were able to predict protection across two additional human challenge studies. Functional validation using monoclonal antibodies confirmed the protective role of Fc-mediated antibody functions in restricting parasite infection both in vitro and in vivo, suggesting that these correlates may mechanistically contribute to parasite restriction and can be used to guide the rational design of an improved vaccine against malaria.

INTRODUCTION

Malaria, a mosquito-borne disease caused by *Plasmodium* spp., was responsible for 405,000 deaths in 2018, with almost an additional 4 billion people at risk of disease (*1*). Although insecticide-treated bed nets, mosquito control, and antimalarial drug distribution programs have substantially reduced mortality associated with the disease, 228 million infections across 87 countries were reported in 2018, disproportionately in African countries (*1*). The development of a vaccine that can block infection is critical to the ultimate eradication of this parasite, particularly in light of the emergence of drug-resistant parasites (*2*–*4*). However, although the malaria vaccine RTS,S/AS01 has demonstrated partial efficacy in phase 3 trials (*5*–*8*) and pilot vaccination programs using RTS,S/AS01 have begun in three countries (*9*), rational vaccine improvement, aimed at driving enhanced protection, have lagged because of our incomplete understanding of the protective immune response against the parasite (*10*).

RTS,S/AS01 is a subunit vaccine consisting of a fusion protein constructed from the central NANP repeat region of *Plasmodium falciparum* circumsporozoite protein (CSP); the C-terminal, T cell epitope–rich region of CSP; and the hepatitis B virus surface antigen, adjuvanted with GlaxoSmithKline's proprietary AS01 adjuvant (liposomes with monophosphoryl lipid A and QS21 purified from the bark of the *Quillaja saponaria* tree) (*11*). In controlled human malaria infection (CHMI) studies, the RTS,S/AS01 vaccine has shown 40 to 80% vaccine efficacy in malaria-naïve individuals (*12*–*17*). The vaccine also showed a 36.3% reduction in clinical malaria and a 32.2% reduction in severe malaria over about 4 years of follow-up in a phase 3 trial in African children receiving a four-dose vaccination regimen who started their vaccination between 5 and 17 months of age (*5*).

[1]Ragon Institute of MGH, Harvard, and MIT, Cambridge, MA 02139, USA. [2]Institute for Medical Engineering and Science, Massachusetts Institute of Technology, Cambridge, MA 02139, USA. [3]Thayer School of Engineering, Dartmouth College, Hanover, NH 03755, USA. [4]PATH's Malaria Vaccine Initiative, Washington, DC 20001, USA. [5]GSK Vaccine, 1300 Wavre, Belgium. [6]Malaria Research Institute, Johns Hopkins Bloomberg School of Public Health, Baltimore, MD 21205, USA. [7]Malaria Vaccine Branch, Walter Reed Army Institute of Research, Silver Spring, MD 20910, USA. [8]Janssen Vaccines & Prevention B.V., 2333CN Leiden, Netherlands. [9]Koch Institute for Integrative Cancer Research, Cambridge, MA 02139, USA. [10]Broad Institute, Cambridge, MA 02139, USA. [11]Howard Hughes Medical Institute, Chevy Chase, MD 20815, USA. [12]Department of Medicine, Brigham and Women's Hospital, Boston, MA 02115, USA. [13]Department of Biological Engineering, Massachusetts Institute of Technology, Cambridge, MA 02139, USA.
*These authors contributed equally to this work.
†Present address: SeromYx Systems, Cambridge, MA 02139, USA.
‡Present address: Center for Systems Immunology, Departments of Immunology and Computational & Systems Biology, University of Pittsburgh School of Medicine, Pittsburgh, PA 15213, USA.
§Corresponding author. Email: galter@mgh.harvard.edu (G.A.); erik.x.jongert@gsk.com (E.J.); uwille-reece@path.org (U.W.-R.)

In CHMI studies, a number of features have been linked to protection from infection, including elevated antibody concentrations (*14*), interferon-γ (IFN-γ) production by immune cells (*18*), phagocytic antibodies targeting the CSP repeat region but not the C-terminal domain (*19*), transcriptional signatures at the time of vaccination (*20*), and both IFN-γ serum concentrations and IFN-γ–related transcriptional signatures on the day of challenge (*21*, *22*). However, each correlate has emerged in a single CHMI study, and the resulting correlates have translated poorly as predictors across additional studies and have not been linked to clearance of parasites or infected cells (*23*–*26*). Thus, further vaccine improvement has been hampered by the absence of a consistent functional correlate across RTS,S CHMI and field studies.

Antibodies are the primary correlates of protection after most clinically approved vaccines (*27*), and antibody concentrations are linked to protection from CHMI after RTS,S/AS01 vaccination (*14*). Beyond simply binding to pathogens, antibodies coordinate the direct destruction of pathogens and infected cells through their ability to activate the innate immune system via binding to Fc receptors, complement, and lectin-like proteins (*28*, *29*). These functional activities of antibodies, including induction of antibody-dependent phagocytosis, antibody-dependent complement deposition, and antibody-dependent cytotoxicity, are increasingly recognized as important in antibody-mediated protection from infection (*30*–*34*). As efforts to improve vaccine-induced immunity, focused on altering vaccine regimens or scheduling, suggest that antibody titers are an imperfect correlate of protection, qualitative (i.e., antibody functionality), rather than quantitative (i.e., antibody titers), differences in vaccine-induced antibodies may play a critical role in protection against malaria. Therefore, we aimed to broadly and comprehensively capture the innate immune–recruiting functions of CSP-specific antibodies across individuals who were protected or became infected after CHMI, focusing on a unique CHMI study where similar frequencies of protection were observed after challenge despite substantial differences in vaccine-elicited antibody concentrations (*14*).

RESULTS

Limited power of individual antibody features in predicting protection after vaccination with RTS,S/AS01

Here, we aimed to deeply profile the functional humoral responses after RTS,S/AS01 vaccination to define potential conserved correlates of protection. We focused on a unique CHMI trial [MAL068; NCT01366534 (*14*)] with two vaccine arms: (i) a three-dose RTS,S/AS01 arm (RRR; n = 21, 11 protected/10 infected) and (ii) an adenovirus 35 (Ad35).PfCSP prime and two doses of RTS,S/AS01 arm (ARR; n = 25, 11 protected/14 infected). Similar frequencies of protection from infection were observed across both groups [ARR: 44%; 95% confidence interval (CI), 21% to 60%; RRR: 52%; 95% CI, 25% to 70%]. Although antibody concentrations were associated with protection from infection within each arm, the magnitude of antibodies induced in the ARR arm were significantly lower than those in the RRR arm (*14*), suggesting that antibody concentrations alone are insufficient to predict protection from infection.

To explore qualitative differences in vaccine-induced antibodies that explain protection from infection, we applied systems serology (*35*) to broadly analyze the biophysical and functional characteristics of vaccine-induced antibodies present in the serum of vaccinated individuals on the day of malarial challenge, 3 weeks after the final vaccination. More than 120 antibody features were measured per subject against full-length CSP, the central NANP repeat region (NANP6), or the C-terminal (Pf16) region of *P. falciparum* (Fig. 1A). These features incorporated both the biophysical characteristics of antigen-specific antibodies, including vaccine-induced antibody isotypes and immunoglobulin G (IgG) subclasses, binding to C1q and Fc receptors, and Fc glycosylation, as well as the functional activity of these antibodies, including the ability to activate natural killer (NK) cells and the complement pathway and induce phagocytosis by various innate immune cell populations. Although differences in antibody functions and features between infected and protected individuals were observed (Fig. 1B and fig. S1), after correction for multiple comparisons, a limited number of features, including antigen-specific antibody binding to activating Fcγ receptors (FcγRs) and activation of NK cells, reached statistical significance ($q < 0.05$), suggesting that specific Fc features and functions may be linked to protection after vaccination with RTS,S/AS01.

RRR-specific multivariate signatures of protection point to the importance of antibody function, rather than quantity alone, in protection from malaria infection

Antibody titers in the RRR group that became infected were equivalent to antibody titers in the protected ARR subjects (*14*). Thus, antibody titer only provides a cursory measurement of the immune parameters associated with protection. Therefore, to begin to define the specific antibody features that track with protection across each vaccine arm, a multivariate model was built. After vaccination, changes in antibody function, subclass selection, and glycosylation occur simultaneously to the evolution of the humoral immune response and the rise in antibody titers (*35*). Thus, to avoid overfitting, a conservative feature downselection methodology [least absolute shrinkage and selection operator (LASSO)] that probes the correlation structure of the overall dataset and then selects the minimal number of features that capture the overall variation in the dataset was applied (*36*). These downselected features were then used in a multivariate classification to determine whether the minimal features could resolve protected vaccinees from those that succumbed to infection after challenge. Focusing initially only on vaccinees in the RRR arm, protected and infected individuals could be accurately separated (Fig. 2A) using a model built on only 2 of the 128 original antibody features (Fig. 2B): repeat region (NANP6)–specific antibodies able to bind to FCGR3A, the activating Fc receptor involved in NK cell activation, and NANP6-specific antibodies able to induce monocyte phagocytosis.

Because LASSO selects a minimal set of predictive markers that each track with additional humoral variables that differ with protection, we further probed the features correlated with the two in the model to gain deeper biological insights into humoral functions that may be important for protection. Network analyses (Fig. 2C) identified a single dense network of nearly entirely repeat region–specific functions and Fc receptor–binding features, linking NANP6-specific antibody binding to FCGR3A directly to antibody-dependent NK cell degranulation and chemokine production. Thus, although FCGR3A can be expressed on additional innate immune cell types, the network clearly illustrated the importance of this feature in marking enhanced NK cell activity as a key functional response linked to protection. In addition, repeat region–specific antibody-dependent cellular phagocytosis (ADCP) activity was linked solely

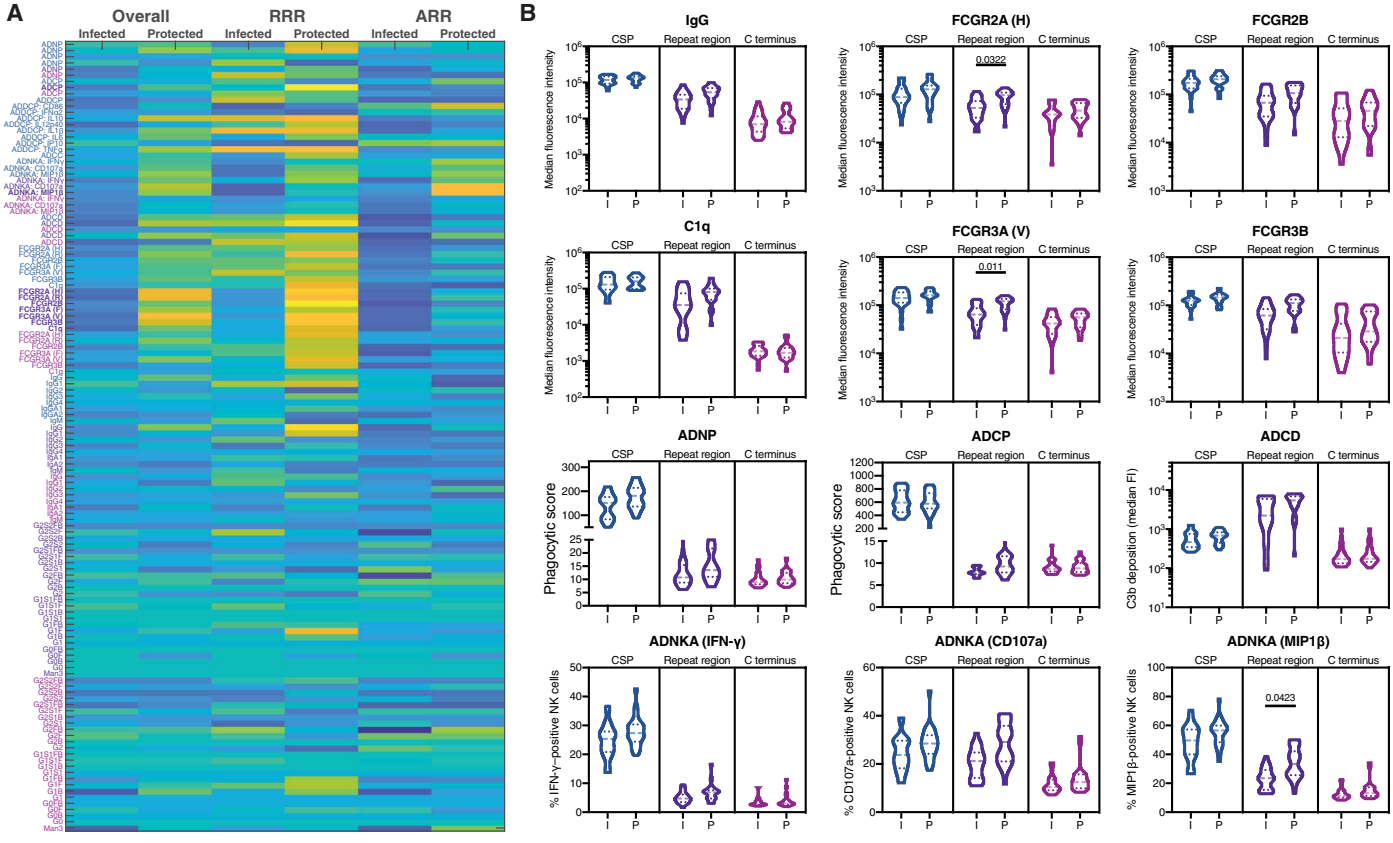

Fig. 1. Univariate profiling of MAL068 vaccinees. (**A**) The heatmap illustrates all systems serology–acquired data. The color indicates the median *Z*-scored value across individuals who went on to become infected or who were protected for all subjects in the MAL068 trial (overall; $n = 46$, 22 protected and 24 infected), RRR vaccinees (middle; $n = 21$, 11 protected and 10 infected), or ARR vaccinees (right; $n = 25$, 11 protected and 14 infected) for CSP-specific (blue text), repeat region–specific (purple text), or C-terminal peptide–specific (pink text) responses. Data were analyzed using a Kruskal-Wallis test followed by a Bonferroni correction for multiple comparisons. Significant features, defined as $q < 0.05$, where q is the P value adjusted for multiple comparisons, are indicated in bold. (**B**) The violin plots illustrate the distribution of the data for a subset of individual features and functions. Median values are indicated with the dashed line, and quartiles are indicated with dotted lines. Data were analyzed using a Mann-Whitney *U* test, and significance was determined after Holm-Šídák correction for multiple comparisons. Corrected *P* values for significant differences are reported. FCGR2A (H), FCGR2A 131H variant; FCGR3A (V), FCGR3A 157V variant; ADNP, antibody-dependent neutrophil phagocytosis; ADCP, antibody-dependent cellular phagocytosis; ADCD, antibody-dependent complement deposition; ADNKA, antibody-dependent NK cell activation.

to neutrophil-mediated phagocytosis, suggesting that these phagocytic functions may be interchangeably elevated among protected individuals. Although the network demonstrates that a minimal set of two vaccine-specific antibody features are sufficient to stratify protected and infected subjects using LASSO/partial least-squares discriminant analysis (PLSDA), it is critical to note that the co-correlate networks represent the entire spectrum of humoral measurements associated with protection. Combined, these data highlight the protective nature of functional, repeat region–specific immune responses in RRR vaccinees. Furthermore, although both features were highly predictive on their own (Fig. 2D), prediction using a linear combination of both variables was more accurate, with a median classification accuracy greater than 90% in a 10-fold cross-validation framework [latent variable 1 (LV1) area under the receiver operating characteristic (AUROC) = 0.91; 75% CI, 0.84 to 0.99] that was further validated using random or permutation testing in a matched cross-validation framework (fig. S2). These results point to the critical importance of antibody functions, specifically binding to FCGR3A and ADCP activity, rather than antibody concentrations alone, as critical predictive biomarkers of protection. Linked to the network analysis highlighting the strong relationship of FCGR3A binding with NK cell functions and ADCP with antibody-dependent neutrophil phagocytosis (ADNP) activity, these data clearly link NK cell, monocyte, and neutrophil activity as critical functional antibody-associated predictors of protection.

ARR-specific multivariate functional signatures, rather than antibody concentrations, associated with protection from malaria infection

Protection in ARR was observed at significantly lower antibody concentrations than those observed in RRR vaccinees in the MAL068 trial (fig. S3; $P = 0.026$) (*14*). Thus, we speculated that the functional profile of antibodies that tracked with protection would vary from those observed in RRR vaccinees. As expected, antibody profiles were not as clearly divergent among protected and infected vaccinees in the ARR arm. However, individuals who were infected clustered more tightly in the PLSDA plot (Fig. 3A). Using feature downselection (LASSO), we were able to build a predictive model using only 5 of the 128 features that, collectively, were able to separate the protected and infected individuals with an AUROC greater than

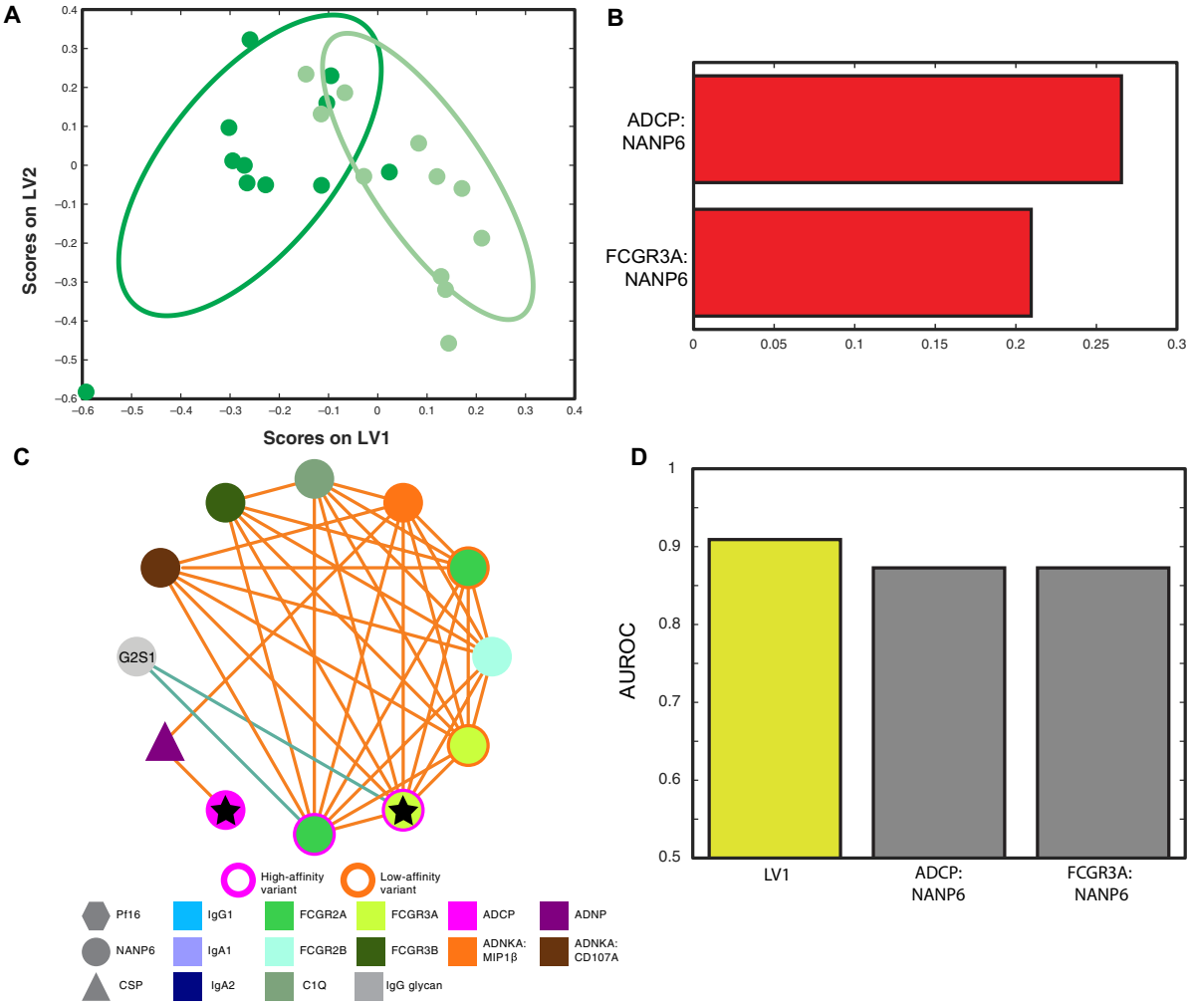

Fig. 2. RRR-specific correlates of protection in the MAL068 study. (**A**) The partial least-squares (PLS) latent variable (LV) score biplot depicts protected (dark shade) and infected individuals (light shade) in the RRR arm; LVs were constructed using LASSO-selected features that stratified vaccinees on the basis of their protection status. Ellipses correspond to 75% confidence intervals (CIs) for each group. (**B**) The bar graphs depict the variable importance scores of the LASSO-selected features that were required to resolve protected and infected individuals in the RRR arms. The magnitude of the bar represents the relative importance of that feature in driving separation, and the color and direction of the bar indicate whether the feature is enriched in protected (red, right) or infected individuals (blue, left). (**C**) The correlation network depicts the antibody features that are significantly correlated with the LASSO-selected, minimal features required to accurately separate protected individuals from infected individuals in the RRR arm. Spearman correlations between all pairs of features were computed, and the significance of the correlations was assessed using the false discovery rate (FDR; i.e., *P* values corrected for multiple comparisons using the Benjamini-Hochberg method). A correlation was defined as significant only if it passed both an effect size threshold ($|r| > 0.7$) and a statistical significance threshold (FDR < 0.01). Networks are centered around the LASSO-selected features (indicated with a star), with the shape of the node corresponding to the antigen (hexagon, Pf16; circle, NANP6; triangle, full-length CSP) and the color of the node corresponding to the antibody feature. Positive correlations are indicated by an orange line, whereas a green line indicates a negative correlation. (**D**) The bar graphs capture the predictive power, defined as the area under the ROC curve (AUROC), for the composite LV1, which is composed of the LASSO/PLS-selected features (yellow) compared to the individual features making up LV1 for the RRR arm. LV1, AUROC: 0.91 (75% CI: 0.84 to 0.99); ADCP:NANP6, AUROC: 0.87 (75% CI: 0.77 to 0.97); FCGR3A:NANP6, AUROC: 0.87 (75% CI: 0.78 to 0.96).

0.85 (Fig. 3B). Two of the five features were directly related to the RRR protective signature. NANP6-specific ADCP activity was associated with protection in both the RRR and ARR arms. In addition, NANP6-specific antibody–mediated activation of chemokine secretion by NK cells was identified as the top correlate in the ARR arm and was linked to NANP6-specific antibody binding to FCGR3A in the RRR network. The remaining three ARR features were uniquely up-regulated in protected individuals in the ARR arm (Pf16-specific IgA2 and IgG2 concentrations and NANP6-specific IgA1 concentrations; Fig. 3B). Network analysis of the identified features resulted in an overall network topology that was very similar to the network observed in the analysis of the RRR arm, with many shared features. Deeper inspection of the co-correlates of the LASSO-selected features again highlighted a dense network of NANP6-specific NK cell features, including binding to FCGR3A and induction of NK cell degranulation, and an enrichment of NANP6-specific IgA signatures among protected individuals (Fig. 3C). Although the individual LASSO-selected features provided variable predictive accuracy alone, a latent variable built on all five features provided robust prediction accuracy (Fig. 3D), statistically outperforming

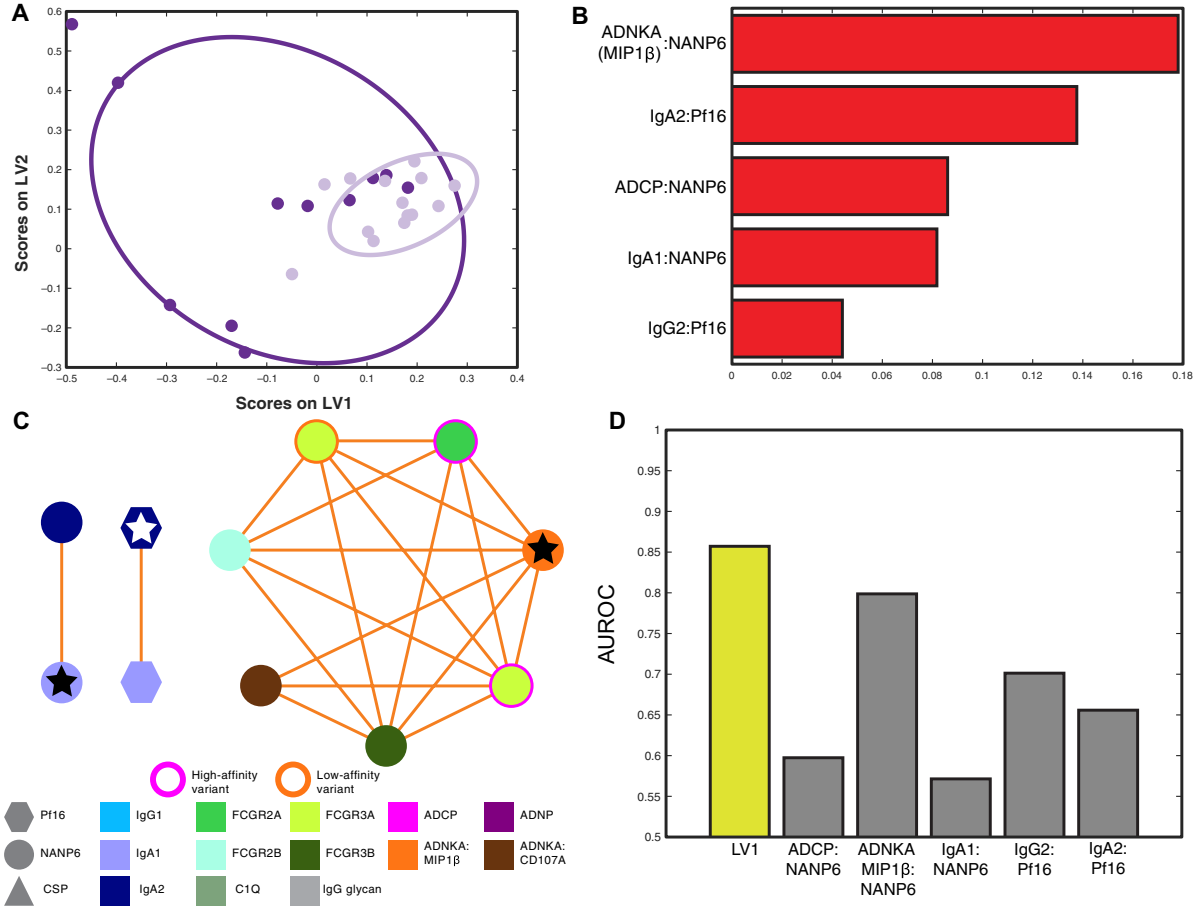

Fig. 3. ARR-specific correlates of protection in the MAL068 study. (**A**) The PLS LV score biplot depicts protected (dark shade) and infected individuals (light shade) in the ARR arm; LVs were constructed using LASSO-selected features that stratified vaccinees on the basis of their protection status. Ellipses correspond to 75% CI for each group. (**B**) The bar graphs depict the variable importance scores of the LASSO-selected features that were required to resolve protected and infected individuals in the ARR arms. The magnitude of the bar represents the relative importance of that feature in driving separation, and the color and direction of the bar indicates whether the feature is enriched in protected (red, right) or infected individuals (blue, left). (**C**) The correlation network depicts the antibody features that are significantly correlated with the LASSO-selected, minimal features required to accurately separate protected individuals from infected individuals in the ARR arm. Spearman correlations between all pairs of features were computed, and the significance of the correlations was assessed using the false discovery rate (i.e., *P* values corrected for multiple comparisons using the Benjamini-Hochberg method). A correlation was defined as significant only if it passed both an effect size threshold ($|r| > 0.7$) and a statistical significance threshold (FDR < 0.01). Networks are centered around the LASSO-selected features (indicated with a star), with the shape of the node corresponding to the antigen (hexagon, PF16; circle, NANP6; triangle, full-length CSP) and the color of the node corresponding to the antibody feature. Positive correlations are indicated by an orange line, whereas a green line indicates a negative correlation. (**D**) The bar graphs capture the predictive power, defined as the AUROC, for the composite LV1, which is composed of the LASSO/PLS-selected features (yellow) compared to the individual features making up LV1 for the ARR arm. LV1, AUROC: 0.86 (75% CI: 0.77 to 0.94); ADCP:NANP6, AUROC: 0.60 (75% CI: 0.45 to 0.76); MIP1β:NANP6, AUROC: 0.80 (75% CI: 0.70 to 0.90); IgA1:NANP6, AUROC: 0.57 (75% CI: 0.44 to 0.71); IgG2:Pf16, AUROC: 0.70 (75% CI: 0.56 to 0.85); IgA2:Pf16, AUROC: 0.66 (75% CI: 0.52 to 0.80).

random or permuted data in a 10-fold cross-validation framework (fig. S4). Thus, these data point again to antibody quality (NK cell activation, phagocytic function, and subclass/isotype selection differences), rather than antibody concentrations, as predictors of protection.

A converging set of humoral correlates predict protection irrespective of vaccine arm

The presence of similar functional predictors of protection across vaccine arms in MAL068 vaccinees pointed to a potential converging functional signature of protection, irrespective of vaccine modality and antibody concentration. To test this hypothesis, data for all vaccinees in the MAL068 trial, irrespective of vaccine arm, were combined and a multivariate model was built after feature down-selection. Despite the differences in antibody concentrations across vaccine arms, a LASSO model built using the vaccine-induced antibody Fc features from the combined arms was able to discriminate protection status (Fig. 4A). Only five features were required to separate protected and infected individuals (Fig. 4B), with a single feature (CSP-specific IgM concentrations) selectively enriched in infected individuals, pointing to a potential marker of susceptibility to infection. The remaining four features were enriched in individuals who were protected, and three of these features were identified in the RRR and ARR analysis (Fig. 4B). Specifically, NANP6-specific antibody binding to FCGR3A, NANP6-specific antibodies able to induce NK cell chemokine secretion, and NANP6-specific antibodies able to

induce phagocytosis were critical discriminators of protected individuals, reinforcing the critical importance of NK cell–like and phagocytic functions in protection against malaria. In addition, C-terminal peptide (Pf16)–specific IgA2 concentrations, a feature previously observed in protected ARR vaccinees, again emerged, pointing to a potentially protective role for antibodies targeting the C-terminal domain of the RTS,S antigen.

Further co-correlates analysis of the LASSO-selected features (Fig. 4C) highlighted isotype-restricted relationships for IgA and IgM, where the protective Pf16-specific IgA2 response was tied to concordantly higher concentrations of Pf16-specific IgA1, highlighting a potential role for pan-IgA–driven Pf16 peptide–specific immune responses in protection against infection. By contrast, the nonprotective CSP-specific IgM signature was associated with repeat region–specific IgM, suggesting that incomplete class switching may function as an indicator of a nonprotective vaccine-induced immune response. Last, the three NANP6-specific antibody features (binding to FCGR3A, NANP6-specific antibody–driven chemokine secretion by NK cells, and NANP6-specific ADCP) were all tightly linked to additional repeat region–specific functional activities (antibody-dependent complement deposition, ADNP, and antibody-dependent NK cell degranulation) and enhanced binding to other FcγRs and complement (Fig. 4C). When examined individually, the features provided limited predictive power; however, LV1, which combines all five features, was able to robustly classify vaccinees by protection status, regardless of arm-specific differences in antibody concentration (Fig. 4D; LV1 AUROC = 0.86, 75% CI, 0.79 to 0.92), again statistically outperforming random or permuted data in a 10-fold cross-validation framework (fig. S5). These results highlight the importance of antibody functional quality as a critical predictor of protection against infection across all vaccinees. Models based exclusively on either CSP- or hepatitis B virus surface antigen–specific antibody concentrations were less robust in classification accuracy compared to models using antibody Fc-associated readouts (figs. S6 and S7). Thus, these data clearly argue for a convergent and consistent titer-independent functional antibody profile associated with protection against malaria in the MAL068 vaccine trial, with FCGR3A/NK cell and phagocytic antibody functions emerging as key predictors of protection.

RRR correlates predict protection across independent studies

The consistent identification of NANP6-specific antibody features within and across both vaccine arms in the MAL068 trial argued for a broader correlate of protection after RTS,S/AS01 vaccination. To test this hypothesis, we next aimed to determine whether the most stringent, minimal set of correlates, derived from the RRR arm, could predict protection in two additional RTS,S CHMI studies. Although these studies were originally focused on the role of adjuvants (MAL027; NCT00075049) (*15*) or changes in vaccine dose/timing (MAL071; NCT01857869) (*13*), both of these trials included an RRR arm identical to that in the MAL068 trial. Thus, these additional arms offered a unique opportunity to evaluate the accuracy of the correlates of protection identified in the RRR arm of the MAL068 study. Using a highly stringent approach where both the correlate identification and model training were done using only data from the RRR arm of the MAL068 study, we tested whether this two-feature model could predict protection for RRR vaccinees in the MAL027 (Fig. 5A) and MAL071 (Fig. 5B) trials. Examined individually, the two features demonstrated complementary predictive power across the additional studies with NANP6-specific antibody binding to FCGR3A providing more predictive power in the MAL027 study and NANP6-specific ADCP activity providing more predictive power in the MAL071 study (Fig. 5C). Critically, despite differences in the overall magnitude, coordination, and structure of the vaccine-induced immune responses across the additional two studies (fig. S8), the two-feature MAL068 RRR signature robustly predicted protection, with AUROCs of 0.83 (75% CI: 0.72 to 0.94; $P = 0.01$) for MAL027 RRR arm and 0.68 (75% CI: 0.52 to 0.83; $P = 0.04$) for MAL071 RRR arm. Beyond simple classification of individuals as infected or protected, the correlates were also tested for their ability to predict time to infection for the three CHMI trials. This model was again built using only the MAL068 data, testing the value of these correlates on MAL027 and MAL071 in a highly stringent cross-prediction on these orthogonal datasets. The correlates were highly predictive of time to infection across the three CHMI trials (Fig. 5D), further confirming the conservation of the functional biomarkers across trials. Collectively, these data suggest that the MAL068 RRR functional humoral correlates have predictive power that extends beyond the MAL068 CHMI trial.

NK cells inhibit in vitro sporozoite invasion in the presence of antibodies

Emerging data point to a potential role for antibodies that are directly cytotoxic (*37*) or directly block sporozoite invasion in protection from infection (*38*–*40*). However, whether antibodies that leverage innate immune effector functions could similarly provide protection against sporozoite infection of hepatocytes is incompletely understood. Specifically, although previous data have demonstrated that antibodies can induce phagocytosis of sporozoites (*41*), it is unclear whether antibody-dependent NK cell activation or phagocytosis could also limit sporozoite infectivity. Thus, we sought to determine whether antibodies cloned from RTS,S/AS01 vaccinees that could induce NK cell degranulation and phagocytosis of sporozoites could restrict *P. falciparum* infection of human hepatocytes in vitro in the presence of innate immune effector cells. Two NANP6-specific antibodies were selected for the analysis (*14*, *42*); MAB311 and MAB250 conferred protection against PfCSP-expressing *Plasmodium berghei* infection in mice (fig. S9A), but only MAB250 was able to block invasion of hepatocytes by *P. falciparum* in vitro (fig. S9B). Both antibodies activated NK cells to a similar degree, with MAB311 inducing more phagocytosis (fig. S9C).

To examine the protective role of innate immune–activating antibodies, a hepatocyte-sporozoite invasion assay (*43*) was modified to include primary NK cells, THP-1 cells (a phagocytic cell line), or primary neutrophils as well as sporozoites and antibodies (Fig. 6, A and B). NK cells were added in a transwell to prevent heterologous hepatocyte lysis, whereas THP-1 cells and neutrophils were added directly to the hepatocytes. In the absence of antibodies, there were no significant differences in the number of intrahepatocyte sporozoites, suggesting that alone, innate immune cells cannot restrict hepatocyte invasion. The addition of MAB250 blocked sporozoite invasion on its own, nearly completely preventing sporozoite infection in the absence of any effector cells. By contrast, MAB311 was unable to block sporozoite invasion of hepatocytes in vitro alone but significantly inhibited hepatocyte infection in the presence of NK cells ($P < 0.001$), THP-1 cells ($P = 0.0360$), or neutrophils ($P = 0.0317$; Fig. 6C). Although previous reports demonstrate that some antibodies are able to prevent sporozoite motility (*40*, *44*), no

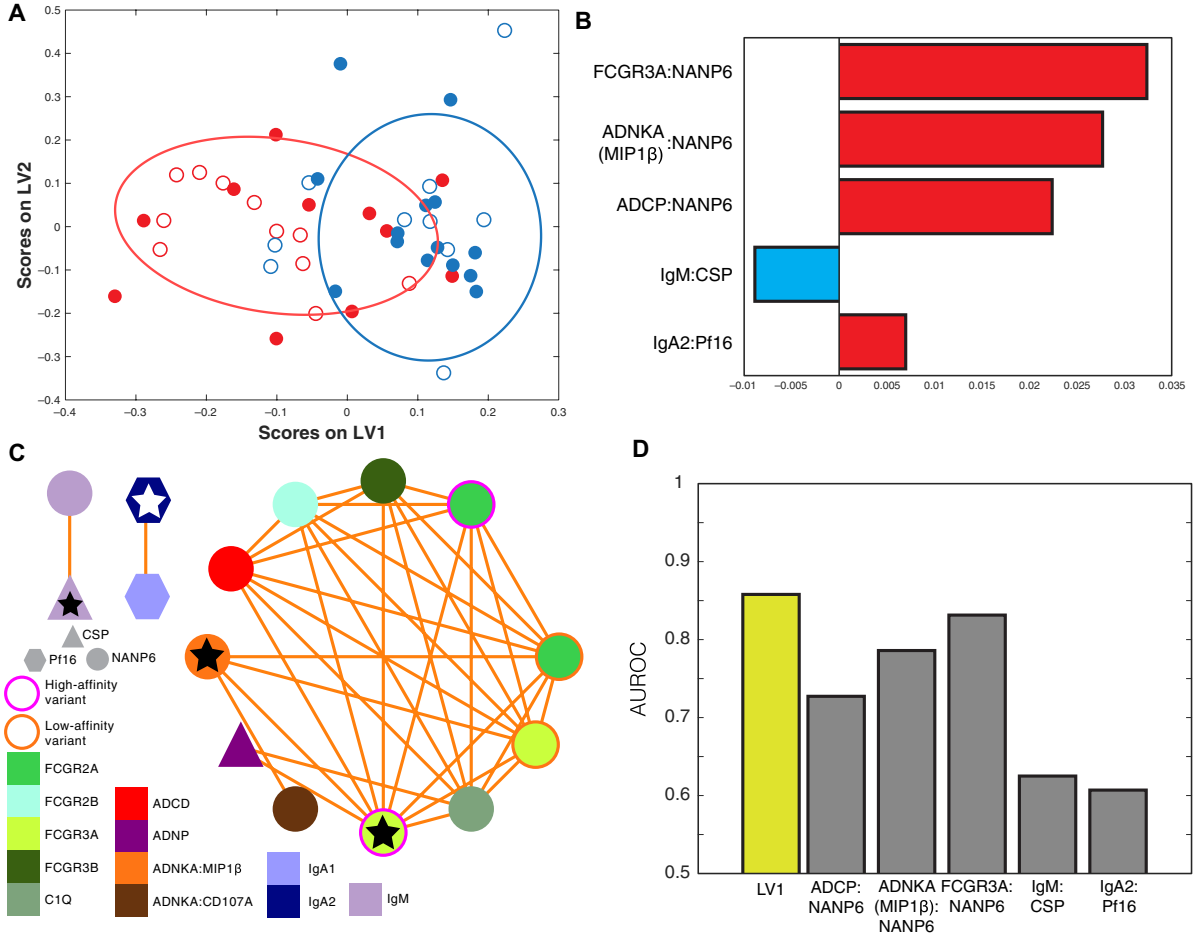

Fig. 4. Defining a single humoral correlate of protection in MAL068 vaccinees. (**A**) Protected (red) and infected (blue) individual can be stratified using a multivariate model. The data are presented as a PLS LV score biplot using LASSO-selected features. Open circles indicate individuals in the RRR arm, whereas filled circles indicate individuals in the ARR arm. Ellipses correspond to 75% CIs. (**B**) The bar graphs depict the variable importance scores of the LASSO-selected features required to stratify individuals by protection status. Blue bars to the left indicate features enriched in infected individuals, whereas red bars to the right indicate features enriched in protected individuals. (**C**) The correlation networks details the antibody features that are significantly correlated with the minimal features required to accurately separate protected individuals from infected individuals. The LASSO-selected features are indicated with a star, and the shape and color of the individual nodes correspond to the antigen and the measured antibody feature, respectively. Positive correlations are indicated by an orange line. (**D**) The predictive power of LV1 (yellow) and the individual features that were used to generate LV1 was quantified as the AUROC curve. LV1, AUROC: 0.86 (75% CI: 0.79 to 0.92); ADCP:NANP6, AUROC: 0.73 (75% CI: 0.64 to 0.82); MIP1β:NANP6, AUROC: 0.79 (75% CI: 0.71 to 0.87); FCGR3A:NANP6, AUROC: 0.83 (75% CI: 0.76 to 0.91); IgM:CSP, AUROC: 0.63 (75% CI: 0.53 to 0.72); IgA2:Pf16, AUROC: 0.61 (75% CI: 0.51 to 0.71).

difference was observed in total sporozoite numbers that crossed the transwell into the hepatocyte chamber in the NK cell assays, as equivalent numbers of sporozoites were observed in the lower chamber under all conditions (fig. S9D). Thus, reduced sporozoite invasion in the presence of antibody and NK cells is likely the result of restriction of sporozoite infectivity, rather than simply retention of sporozoite-immune complexes in the presence of antibody. These data suggest that antibodies capable of leveraging an array of innate immune effectors do not simply block sporozoite transit but directly restrict hepatocyte infection. In further support of these findings and given the unexpected influence of NK cells in sporozoite restriction, scanning electron microscopy revealed direct interactions between NK cells and sporozoites in the presence of antibodies (Fig. 6D), and NK cells readily degranulated in vitro in response to sporozoites in the presence of antibodies (Fig. 6E). Last, to further demonstrate the importance of Fc-mediated antibody effector functions in the in vivo protection afforded by MAB311, an Fc variant that lacked all antibody functionality (N297Q) was generated, and the ability of this variant to prevent infection of mice with *P. berghei* sporozoites expressing *P. falciparum* CSP was compared to wild-type MAB311 (Fig. 6F). Whereas wild-type MAB311 effectively restricted infection (average reduction in parasite burden = 84.6%), ablation of Fc-mediated antibody function with the N297Q mutation resulted in a significant decrease in the protection afforded by MAB311 (average reduction in parasite burden = 54.6%, $P = 0.0079$). Combined, these data highlight the potential mechanistic role for Fc-leveraged innate immune cell–activating antibody functions as mechanistic contributors to the prevention of infection and not just as simple biomarkers of protection after RTS,S/AS01 vaccination.

DISCUSSION

Despite a clear role for antibodies in protection against malaria infection after RTS,S vaccination, antibody concentrations are

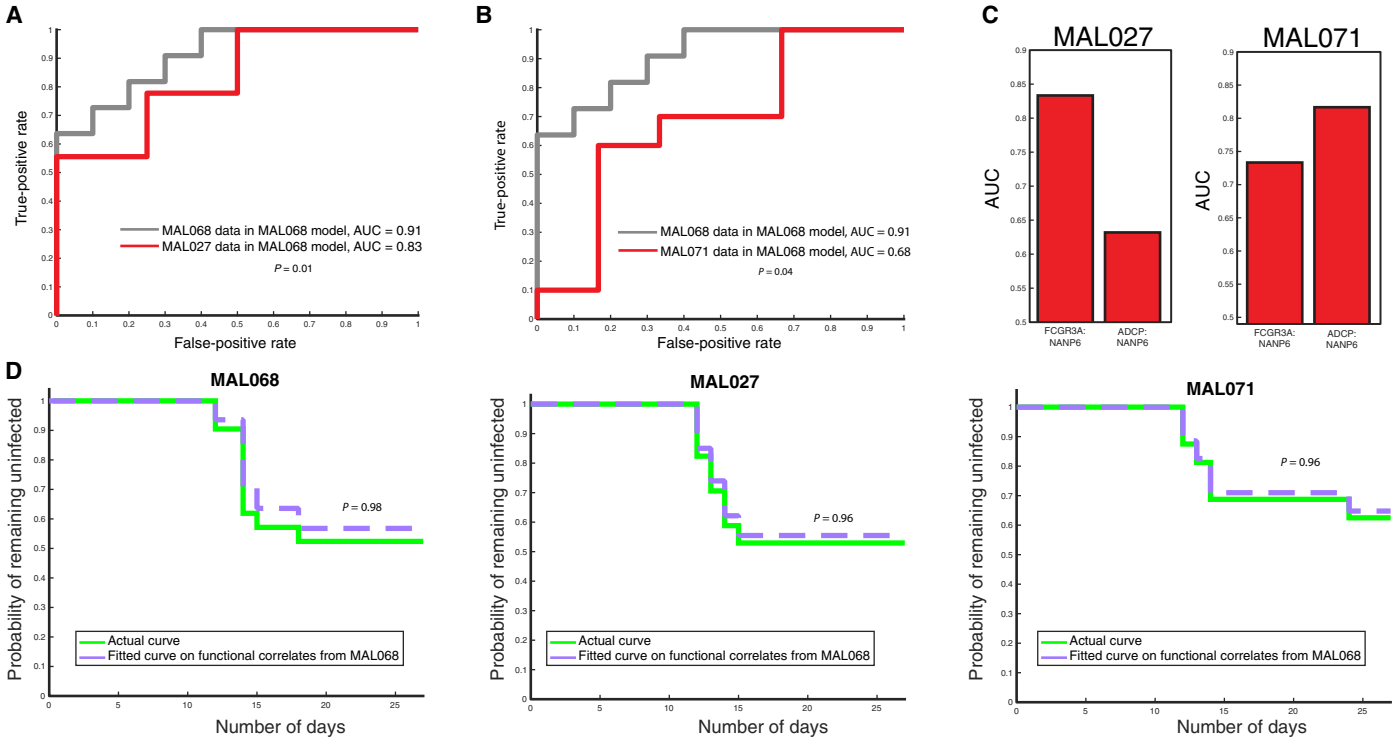

Fig. 5. The MAL068 RRR arm–derived correlates can accurately predict protection in other RTS,S/AS01 CHMI studies. (**A** and **B**) The AUROC curves show the predictive power of a two-feature model (NANP6-specific ADCP and NANP6-specific antibody binding to FCGR3A) derived from the RRR arm of the MAL068 study for the RRR arms of the (A) MAL027 and (B) MAL071 studies. Both correlate identification and model training were done using data only from the RRR arm of the MAL068 trial; no data from the MAL027 or MAL071 studies were used for model training. (**C**) The bar graphs show the differential predictive power of the MAL068-derived features in the MAL071 and MAL027 studies. The predictive power of the individual features that were used to generate the MAL068 model for the RRR arm of the MAL068, MAL027, and MAL071 studies was quantified as the AUROC. (**D**) The curves illustrate the actual and predicted/fitted infection curves for MAL068, MAL027, and MAL071. The predicted infection curves were generated using the correlates identified in the MAL068 study (FCGR3A:NANP6 and ADCP:NANP6). AUC, area under the curve.

inconsistently associated with protection. A consistent correlate of immunity, able to reproducibly predict protection across vaccine studies, could substantially accelerate vaccine development. Both natural and vaccine-induced immunity to *Plasmodium* spp. has been associated with diverse antibody effector functions (*19*, *37*, *45*, *46*). Specifically, individual studies have linked phagocytic functions to vaccine-mediated pre-erythrocytic protection (*14*), whereas neutrophils, complement, opsonophagocytic, and NK cell–activating antibodies have all been linked to blood stage protection (*45*, *47*–*49*). As mentioned above, in some studies, antibody concentrations have been associated with RTS,S-induced protection, and IFN-γ enzyme-linked immunospot and CD4 T cell responses have also provided enhanced resolution of protection in CHMI trials exploring the utility of adjuvants (*24*). Subsequent work pointed to the critical role of IFN-γ and NK cell signatures in protected vaccinees (*21*, *22*). Moreover, evidence that interleukin-2–producing CD4 T cells could stimulate NK cells to produce IFN-γ led to a hypothesized role for NK cells in RTS,S/AS01-induced protection (*21*, *22*). However, the specific mechanism(s) by which NK cells could be selectively leveraged to drive protection remained unclear. The data presented here reconcile this large body of work, providing a mechanistic bridge by which vaccine-induced NK cell–activating antibodies appear to provide specificity to NK cells, as well as other innate immune players, to drive parasitic clearance. Whether NK cells are also tuned after vaccination to become more responsive to these antibodies, in an autologous plasma/NK cell system, is unknown, but collectively, the data argue for a critical role for innate immune–recruiting antibodies in protection against infection after RTS,S vaccination.

Given that antibody functions are likely to be co-correlated, a penalty-based LASSO-driven feature reduction approach was used to select the minimal number of features that could account for the greatest level of variance across the dataset. Ultimately, only two key features, ADCP (linked to ADNP) and FCGR3A binding (linked to NK cell activity), were identified as key predictors of protection in MAL068 RRR vaccinees, and these features were also associated with protection in ARR vaccinees. Previous analyses have suggested a protective role for NANP6-specific antibodies in the MAL068 RRR vaccinees and a deleterious association with Pf16-specific phagocytosis (*19*). Whereas this association was not observed here, this inconsistency is likely due to the to the modeling approach that was used in the previous study in which Pf16-specific phagocytic activity was inferred by dividing CSP-specific phagocytosis by titers to the different RTS,S epitopes rather than by directly measuring epitope-specific antibody functions. These discrepancies emphasize the critical importance of measuring epitope-specific functionality, rather than simple antibody concentrations, in future malaria vaccine studies to fully deconvolute the nature of the protective immune response to malaria.

However, beyond the previous support for a role for NANP-specific ADCP activity in RTS,S-induced protection (*19*), the data presented

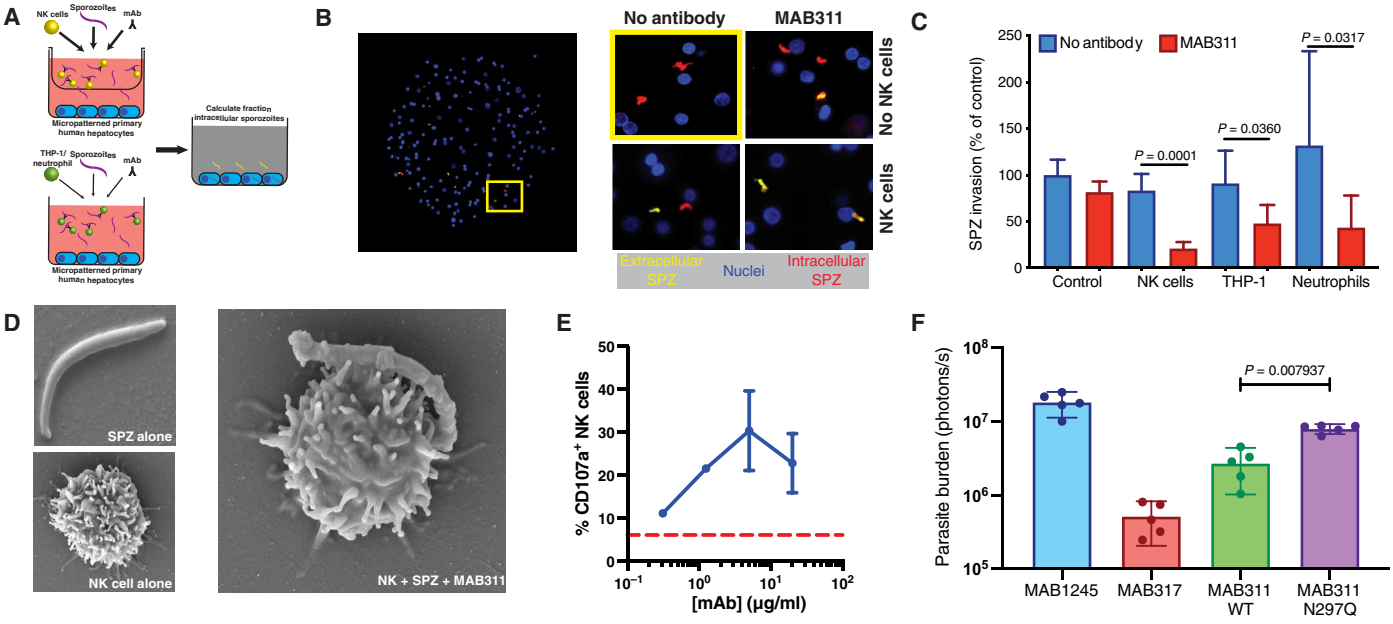

Fig. 6. Antibodies can restrict in vitro sporozoite invasion in the presence of NK cells. (**A**) The schematic depicts the in vitro sporozoite (SPZ) invasion assay. For experiments testing the impact of NK cells and antibodies on sporozoite invasion of hepatocytes, NK cells were separated from the nonautologous hepatocytes with a transwell; primary NK cells, antibodies, and sporozoites were added to the upper chamber of a transwell, incubated, and centrifuged. For experiments testing the impact of neutrophils and monocytes, primary nonautologous neutrophils or THP-1 cells, antibodies, and sporozoites were added directly to the hepatocyte cultures. (**B**) The immunofluorescence images capture the readouts of the in vitro sporozoite invasion assay. Yellow indicates extracellular sporozoites; red indicates intracellular sporozoites, and blue indicates hepatocyte nuclei. (**C**) The bar graph represents the magnitude of in vitro sporozoite invasion in the presence of antibodies and primary NK cells, a monocytic cell line (THP-1), or primary neutrophils. Sporozoite invasion was quantified as the percentage of intracellular sporozoites detected via immunofluorescence normalized to the control [no monoclonal antibody (mAb) and no innate effector cells] for each experiment (run in duplicate across three separate experiments run for each innate immune effector cell). The data are presented as means ± 95% CI. Data were analyzed using a Mann-Whitney *U* test. (**D**) The images represent scanning electron microscopy of NK cells and sporozoites in the presence and absence of MAB311. (**E**) The line graph depicts the proportion of NK cells that degranulated (surface $CD107a^+$) in response to coculture with sporozoites and antibodies in vitro. The data are presented as means ± SE. The dotted red line indicates NK cell degranulation in response to sporozoites and a control human IgG1 antibody at 20 μg/ml. Antibodies were tested in triplicate using two different primary NK cell donors. (**F**) The bar graph depicts the whole-body parasite burden of mice ($n = 5$ per group) treated with monoclonal antibodies before inoculation with *P. berghei* sporozoites expressing *P. falciparum* CSP and green fluorescent protein luciferase and analyzed 42 hours after infection. The data are presented as means ± 95% CI. Data were analyzed using a Mann-Whitney *U* test. WT, wild type.

here also strongly implicate a collaborative role for NK cells and phagocytes, potentially working in a complementary manner, in protection against the parasite. Although the combination of the two features only provided a small increase in prediction accuracy of protection for MAL068 vaccinees, the LASSO model selected both features despite the penalty associated with adding an additional feature. Thus, these functional features likely captured distinct levels of variability in antibody profiles across all vaccinees. The importance of this variability in vaccine-induced immune responses was most apparent in the study cross-validation analysis, where each functional feature provided complementary predictive power across the MAL027 and MAL071 trials (i.e., high/low in one or the other study). Given the complementary importance of both FCGR3A and FCGR2A in driving NK cell and phagocytic function, respectively, these data point to the importance of vaccine-induced antibody recruitment of multiple functions to ensure complete sporozoite eradication and prevention of infection.

Transit of the parasite from the site of infection to the liver occurs rapidly, with the traversal from the skin to the liver occurring in as few as 20 min (*50*, *51*). Thus, skin-resident phagocytic cells, blood monocytes, and liver-resident phagocytic cells could contribute to the rapid and effective clearance of antibody-opsonized sporozoites. Reports that FCGR3A is expressed on subsets of effector memory $CD8^+$ T cells (*52*), $CD8^+$ mucosal-associated invariant T cells (*53*), and $CD56^+CD3^+$ NKT-like cells (*54*) suggest that antibody-dependent restriction of sporozoites could also be mediated by additional peripheral or liver-resident T cell populations. However, the role of NK cells in sporozoite control has been raised but was more controversial (*20*, *55*). Although less abundant than neutrophils or monocytes in the blood, circulating NK cells are remarkably effective in eliminating antibody-opsonized pathogens upon contact. Moreover, NK cells account for up to 50% of liver-resident lymphocytes, representing a highly enriched effector cell population poised to attack antibody-opsonized sporozoites arriving in the liver (*56*). However, given that NK cells, neutrophils, and monocytes all had some effect in limiting sporozoite invasion in vitro, these data argue that a collective of innate immune cells may rapidly respond to antibody-opsonized parasites that, if decorated with the correctly functionalized antibodies, may be highly vulnerable to attack and destruction. Direct killing of sporozoites by NK cells has not been previously observed, possibly because of the lack of investigation into a role for antibodies in leveraging NK cell activity against sporozoites. Instead, NK cells have been shown to play an important role in the direct elimination of other human parasites, including

Toxoplasma gondii (*57*), *Cryptosporidium* spp. (*58*), *Leishmania* spp. (*59*), and blood-stage *P. falciparum* (*45*). Here, we demonstrate antibody-directed interactions between NK cells and sporozoites that led to inhibition of sporozoite invasion in vitro and tracked with protection in a mouse model. Although the assay used here only interrogates the antiparasitic function of NK cells on free sporozoites, it is also plausible that antibodies may also target infected hepatocytes for elimination by liver-resident NK cells, thereby preventing infection at both the prehepatic and pre-erythrocytic stages of the disease.

Similar to previous immune correlates analyses performed in the phase 3 vaccine trial, where, in addition to titer (*25*), parasite genomic variation (*60*), measures of antibody avidity (*61*), and IgG subclass selection (*62*) have been recently shown to associate with protection in immunized infants in Africa, the data presented here from CHMI studies highlight the importance of antibody quality as a critical biomarker of effective immunity to malaria. However, whether the CHMI correlates identified here will associate with protection in the field is of great interest, given the critical differences between the phase 3 study in children and malaria-naïve adult participants in CHMI studies, including differences in endemic exposure (*63*) and geography-associated changes in the composition of the immune system in children, particularly in the humoral immune response (*64*). Given our emerging appreciation for the robust activity of NK cells in the first weeks/months of life (*65*), at a time when other immune subsets are dysfunctional (*66*, *67*), it is plausible that NK cell–activating antibodies may provide a critical barrier for invading pathogens in this vulnerable population. However, despite these differences in field and CHMI studies, CHMI studies still provide great value. Although animal models have been used extensively for decades to shape the development of vaccines, providing a clean in vivo system for immune dissection and further therapeutic refinement, these animal models have provided less progress for some pathogens (e.g., malaria, typhoid, shigella, and tuberculosis). The CHMI model provides an indispensable advance, specifically allowing the rapid testing of novel products, safely, in the model that matters most, humans. Coupled with advanced immune profiling techniques, these trials now offer an opportunity to profile the specific correlates of immunity after these interventions to downselect assays, perhaps, for phase 3 testing, or to help develop mechanistic hypotheses to rationally design products that may have greater efficacy in the field.

Given our emerging understanding of the role of adjuvants in shaping the subclass/isotype and glycosylation profiles of vaccine-induced antibodies (*68*), opportunities to tune antibody function are clearly within sight. The data presented here argue that functional properties of vaccine-induced antibodies, rather than IgG concentrations alone, represent critical predictors of protection from infection with *Plasmodium* spp. With the emerging ease to validate the assays used to test ADCP, FCGR3A binding, and NK cell activity of vaccine-induced antibodies, the rational design of next-generation vaccines against malaria may be powered by immune correlates. Whereas the study presented here reached across three separate CHMI studies to define and confirm correlates of immunity, these correlates were established and validated using a single parasite strain and malaria-naïve individuals. Ultimately, defining field-specific correlates in malaria-endemic regions with multiple circulating strains, particularly in children who suffer the majority of disease, is absolutely essential. Thus, systems serology profiling, using complementary field and controlled human challenge models, may provide an opportunity to overcome biases and define common, overarching correlates that may effectively guide the development of vaccines to prevent malaria or other diseases.

MATERIALS AND METHODS

Study design

The goal of this study was to use antibody Fc functional profiling methods to identify immune correlates of protection against controlled malaria challenge after vaccination with RTS,S/AS01. Serum samples were obtained from a phase 2 clinical trial in which subjects were primed with either RTS,S/AS01 or Ad35.PfCSP, boosted with two monthly doses of RTS,S/AS01, and challenged 3 weeks later with malaria-infected mosquitoes. Blood was drawn for serologic analysis before vaccination and immediately before controlled malaria challenge. High-throughput biophysical and immune functional assays were used to measure more than 120 humoral immune features per serum sample. For each assay, serum samples were tested in technical or biological duplicates, as specified in Supplementary Materials and Methods. Experimenters were blinded as to the vaccine group and protection status for each sample until all data had been collected. Machine learning methods (PLSDA and LASSO) were then used to analyze this high-dimensional dataset and identify correlates of protection within each vaccine arm. We similarly analyzed the vaccine-induced antibody responses in subjects from two additional phase 2 trials in which participants received three monthly doses of the RTS,S/AS01 vaccine before controlled challenge. We then assessed the cross-cohort predictive power of our computational model using these additional datasets. To further explore the antibody Fc-dependent effector functions that correlated with protection in our serologic analyses, we tested the ability of CSP-specific monoclonal antibodies to inhibit sporozoite infection of human hepatocytes in vitro in the presence of human innate immune cells. We also tested the ability of an aglycosylated, functionally inert (non–FcγR-binding), CSP-specific monoclonal antibody to inhibit sporozoite infection in mice. Primary data are reported in data file S1.

Statistical analysis

Nonparametric tests were used to assess statistical significance throughout the study. When comparing differences between two groups, the Mann-Whitney *U* test was used with a Holm-Šídák correction for multiple comparisons. When comparing differences between three or more groups, the Kruskal-Wallis test was used with a Bonferroni correction for multiple comparisons. PLSDA and LASSO were used to identify antibody features that best predict protection status. The significance of these predictive models was assessed by comparing them to control models based on either permuted data or randomly selected antibody features, in a 10-fold cross-validation framework, as described in the Supplementary Materials. *P* values were computed as the tail probability of the true classification accuracy in the distribution of control model classification accuracies. The median *P* values across the independent cross-validation replicates were reported. For each of these statistical tests, differences were considered significant if *P* value or *q* value is <0.05. Correlation networks were generated to depict additional antibody features that correlate strongly with the LASSO-selected features that best predict protection status or discriminate between

vaccine arms. Antibody features were included in these networks only if they passed both an effect size threshold (those with |Spearman r_s| > 0.7) and a more stringent statistical significance threshold (false discovery rate < 0.01). The code used for the identification and evaluation of correlates is provided in data file S2.

SUPPLEMENTARY MATERIALS

stm.sciencemag.org/cgi/content/full/12/553/eabb4757/DC1
Materials and Methods
Fig. S1. Univariate humoral immune response comparisons across MAL068 vaccinees.
Fig. S2. Model performance in RRR vaccinees.
Fig. S3. Different concentrations of CSP-specific antibodies track with protection within arms.
Fig. S4. Model performance in ARR vaccinees.
Fig. S5. Performance of model separating protected from infected vaccinees, independent of vaccine arm in the MAL068 study.
Fig. S6. Measurement of antibody concentrations alone cannot predict protection in the MAL068 study.
Fig. S7. Measurement of hepatitis B virus–specific antibody concentrations cannot predict protection in the MAL068 study.
Fig. S8. Architecture of immune responses in individuals vaccinated with RTS,S/AS01 across studies.
Fig. S9. In vitro and in vivo activity of CSP-specific monoclonal antibodies.
Data file S1. Primary data.
Data file S2. Analysis code.
References (*69*–*91*)

View/request a protocol for this paper from *Bio-protocol*.

REFERENCES AND NOTES

1. World Health Organization, *World Malaria Report 2019* (World Health Organizatio, 2019).
2. A. M. Dondorp, F. M. Smithuis, C. Woodrow, L. V. Seidlein, How to contain artemisinin- and multidrug-resistant falciparum malaria. *Trends Parasitol.* **33**, 353–363 (2017).
3. A. O. Talisuna, C. Karema, B. Ogutu, E. Juma, J. Logedi, A. Nyandigisi, M. Mulenga, W. F. Mbacham, C. Roper, P. J. Guerin, U. D'Alessandro, R. W. Snow, Mitigating the threat of artemisinin resistance in Africa: Improvement of drug-resistance surveillance and response systems. *Lancet Infect. Dis.* **12**, 888–896 (2012).
4. A. P. Phyo, S. Nkhoma, K. Stepniewska, E. A. Ashley, S. Nair, R. McGready, C. ler Moo, S. Al-Saai, A. M. Dondorp, K. M. Lwin, P. Singhasivanon, N. P. Day, N. J. White, T. J. Anderson, F. Nosten, Emergence of artemisinin-resistant malaria on the western border of Thailand: A longitudinal study. *Lancet* **379**, 1960–1966 (2012).
5. RTS,S Clinical Trials Partnership, Efficacy and safety of RTS,S/AS01 malaria vaccine with or without a booster dose in infants and children in Africa: Final results of a phase 3, individually randomised, controlled trial. *Lancet* **386**, 31–45 (2015).
6. RTS,S Clinical Trials Partnership, Efficacy and safety of the RTS,S/AS01 malaria vaccine during 18 months after vaccination: A phase 3 randomized, controlled trial in children and young infants at 11 African sites. *PLOS Med.* **11**, e1001685 (2014).
7. RTS,S Clinical Trials Partnership, S. T. Agnandji, B. Lell, J. F. Fernandes, B. P. Abossolo, B. G. Methogo, A. L. Kabwende, A. A. Adegnika, B. Mordmuller, S. Issifou, P. G. Kremsner, J. Sacarlal, P. Aide, M. Lanaspa, J. J. Aponte, S. Machevo, S. Acacio, H. Bulo, B. Sigauque, E. Macete, P. Alonso, S. Abdulla, N. Salim, R. Minja, M. Mpina, S. Ahmed, A. M. Ali, A. T. Mtoro, A. S. Hamad, P. Mutani, M. Tanner, H. Tinto, U. D'Alessandro, H. Sorgho, I. Valea, B. Bihoun, I. Guiraud, B. Kabore, O. Sombie, R. T. Guiguemde, J. B. Ouedraogo, M. J. Hamel, S. Kariuki, M. Oneko, C. Odero, K. Otieno, N. Awino, M. McMorrow, V. Muturi-Kioi, K. F. Laserson, L. Slutsker, W. Otieno, L. Otieno, N. Otsyula, S. Gondi, A. Otieno, V. Owira, E. Oguk, G. Odongo, J. B. Woods, B. Ogutu, P. Njuguna, R. Chilengi, P. Akoo, C. Kerubo, C. Maingi, T. Lang, A. Olotu, P. Bejon, K. Marsh, G. Mwambingu, S. Owusu-Agyei, K. P. Asante, K. Osei-Kwakye, O. Boahen, D. Dosoo, I. Asante, G. Adjei, E. Kwara, D. Chandramohan, B. Greenwood, J. Lusingu, S. Gesase, A. Malabeja, O. Abdul, C. Mahende, E. Liheluka, L. Malle, M. Lemnge, T. G. Theander, C. Drakeley, D. Ansong, T. Agbenyega, S. Adjei, H. O. Boateng, T. Rettig, J. Bawa, J. Sylverken, D. Sambian, A. Sarfo, A. Agyekum, F. Martinson, I. Hoffman, T. Mvalo, P. Kamthunzi, R. Nkomo, T. Tembo, G. Tegha, M. Tsidya, J. Kilembe, C. Chawinga, W. R. Ballou, J. Cohen, Y. Guerra, E. Jongert, D. Lapierre, A. Leach, M. Lievens, O. Ofori-Anyinam, A. Olivier, J. Vekemans, T. Carter, D. Kaslow, D. Leboulleux, C. Loucq, A. Radford, B. Savarese, D. Schellenberg, M. Sillman, P. Vansadia, A phase 3 trial of RTS,S/AS01 malaria vaccine in African infants. *N. Engl. J. Med.* **367**, 2284–2295 (2012).
8. RTS,S Clinical Trials Partnership, S. T. Agnandji, B. Lell, S. S. Soulanoudjingar, J. F. Fernandes, B. P. Abossolo, C. Conzelmann, B. G. Methogo, Y. Doucka, A. Flamen, B. Mordmuller, S. Issifou, P. G. Kremsner, J. Sacarlal, P. Aide, M. Lanaspa, J. J. Aponte, A. Nhamuave, D. Quelhas, Q. Bassat, S. Mandjate, E. Macete, P. Alonso, S. Abdulla, N. Salim, O. Juma, M. Shomari, K. Shubis, F. Machera, A. S. Hamad, R. Minja, A. Mtoro, A. Sykes, S. Ahmed, A. M. Urassa, A. M. Ali, G. Mwangoka, M. Tanner, H. Tinto, U. D'Alessandro, H. Sorgho, I. Valea, M. C. Tahita, W. Kabore, S. Ouedraogo, Y. Sandrine, R. T. Guiguemde, J. B. Ouedraogo, M. J. Hamel, S. Kariuki, C. Odero, M. Oneko, K. Otieno, N. Awino, J. Omoto, J. Williamson, V. Muturi-Kioi, K. F. Laserson, L. Slutsker, W. Otieno, L. Otieno, O. Nekoye, S. Gondi, A. Otieno, B. Ogutu, R. Wasuna, V. Owira, D. Jones, A. A. Onyango, P. Njuguna, R. Chilengi, P. Akoo, C. Kerubo, J. Gitaka, C. Maingi, T. Lang, A. Olotu, B. Tsofa, P. Bejon, N. Peshu, K. Marsh, S. Owusu-Agyei, K. P. Asante, K. Osei-Kwakye, O. Boahen, S. Ayamba, K. Kayan, R. Owusu-Ofori, D. Dosoo, I. Asante, G. Adjei, G. Adjei, D. Chandramohan, B. Greenwood, J. Lusingu, S. Gesase, A. Malabeja, O. Abdul, H. Kilavo, C. Mahende, E. Liheluka, M. Lemnge, T. Theander, C. Drakeley, D. Ansong, T. Agbenyega, S. Adjei, H. O. Boateng, T. Rettig, J. Bawa, J. Sylverken, D. Sambian, A. Agyekum, L. Owusu, F. Martinson, I. Hoffman, T. Mvalo, P. Kamthunzi, R. Nkomo, A. Msika, A. Jumbe, N. Chome, D. Nyakuipa, J. Chintedza, W. R. Ballou, M. Bruls, J. Cohen, Y. Guerra, E. Jongert, D. Lapierre, A. Leach, M. Lievens, O. Ofori-Anyinam, J. Vekemans, T. Carter, D. Leboulleux, C. Loucq, A. Radford, B. Savarese, D. Schellenberg, M. Sillman, P. Vansadia, First results of phase 3 trial of RTS,S/AS01 malaria vaccine in African children. *N. Engl. J. Med.* **365**, 1863–1875 (2011).
9. P. Adepoju, RTS,S malaria vaccine pilots in three African countries. *Lancet* **393**, 1685 (2019).
10. I. A. Cockburn, R. A. Seder, Malaria prevention: From immunological concepts to effective vaccines and protective antibodies. *Nat. Immunol.* **19**, 1199–1211 (2018).
11. J. Vekemans, A. Leach, J. Cohen, Development of the RTS,S/AS malaria candidate vaccine. *Vaccine* **27** (Suppl. 6), G67–G71 (2009).
12. T. Rampling, K. J. Ewer, G. Bowyer, C. M. Bliss, N. J. Edwards, D. Wright, R. O. Payne, N. Venkatraman, E. de Barra, C. M. Snudden, I. D. Poulton, H. de Graaf, P. Sukhtankar, R. Roberts, K. Ivinson, R. Weltzin, B. Y. Rajkumar, U. Wille-Reece, C. K. Lee, C. F. Ockenhouse, R. E. Sinden, S. Gerry, A. M. Lawrie, J. Vekemans, D. Morelle, M. Lievens, R. W. Ballou, G. S. Cooke, S. N. Faust, S. Gilbert, A. V. Hill, Safety and high level efficacy of the combination malaria vaccine regimen of RTS,S/AS01B with chimpanzee adenovirus 63 and modified vaccinia ankara vectored vaccines expressing ME-TRAP. *J. Infect. Dis.* **214**, 772–781 (2016).
13. J. A. Regules, S. B. Cicatelli, J. W. Bennett, K. M. Paolino, P. S. Twomey, J. E. Moon, A. K. Kathcart, K. D. Hauns, J. L. Komisar, A. N. Qabar, S. A. Davidson, S. Dutta, M. E. Griffith, C. D. Magee, M. Wojnarski, J. R. Livezey, A. T. Kress, P. E. Waterman, E. Jongert, U. Wille-Reece, W. Volkmuth, D. Emerling, W. H. Robinson, M. Lievens, D. Morelle, C. K. Lee, B. Yassin-Rajkumar, R. Weltzin, J. Cohen, R. M. Paris, N. C. Waters, A. J. Birkett, D. C. Kaslow, W. R. Ballou, C. F. Ockenhouse, J. Vekemans, Fractional third and fourth dose of RTS,S/AS01 malaria candidate vaccine: A phase 2a controlled human malaria parasite infection and immunogenicity study. *J. Infect. Dis.* **214**, 762–771 (2016).
14. C. F. Ockenhouse, J. Regules, D. Tosh, J. Cowden, A. Kathcart, J. Cummings, K. Paolino, J. Moon, J. Komisar, E. Kamau, T. Oliver, A. Chhoeu, J. Murphy, K. Lyke, M. Laurens, A. Birkett, C. Lee, R. Weltzin, U. Wille-Reece, M. Sedegah, J. Hendriks, I. Versteege, M. G. Pau, J. Sadoff, Y. Vanloubbeeck, M. Lievens, D. Heerwegh, P. Moris, Y. G. Mendoza, E. Jongert, J. Cohen, G. Voss, W. R. Ballou, J. Vekemans, Ad35.CS.01-RTS,S/AS01 heterologous prime boost vaccine efficacy against sporozoite challenge in healthy malaria-naive adults. *PLOS ONE* **10**, e0131571 (2015).
15. K. E. Kester, J. F. Cummings, O. Ofori-Anyinam, C. F. Ockenhouse, U. Krzych, P. Moris, R. Schwenk, R. A. Nielsen, Z. Debebe, E. Pinelis, L. Juompan, J. Williams, M. Dowler, V. A. Stewart, R. A. Wirtz, M. C. Dubois, M. Lievens, J. Cohen, W. R. Ballou, D. G. Heppner Jr.; RTS,S Vaccine Evaluation Group, Randomized, double-blind, phase 2a trial of falciparum malaria vaccines RTS,S/AS01B and RTS,S/AS02A in malaria-naive adults: Safety, efficacy, and immunologic associates of protection. *J. Infect. Dis.* **200**, 337–346 (2009).
16. K. E. Kester, J. F. Cummings, C. F. Ockenhouse, R. Nielsen, B. T. Hall, D. M. Gordon, R. J. Schwenk, U. Krzych, C. A. Holland, G. Richmond, M. G. Dowler, J. Williams, R. A. Wirtz, N. Tornieporth, L. Vigneron, M. Delchambre, M. A. Demoitie, W. R. Ballou, J. Cohen, D. G. Heppner Jr.; RTS,S Malaria Vaccine Evaluation, Phase 2a trial of 0, 1, and 3 month and 0, 7, and 28 day immunization schedules of malaria vaccine RTS,S/AS02 in malaria-naive adults at the Walter Reed Army Institute of Research. *Vaccine* **26**, 2191–2202 (2008).
17. K. E. Kester, D. A. McKinney, N. Tornieporth, C. F. Ockenhouse, D. G. Heppner Jr., T. Hall, B. T. Wellde, K. White, P. Sun, R. Schwenk, U. Krzych, M. Delchambre, G. Voss, M. C. Dubois, R. A. Gasser Jr., M. G. Dowler, M. O'Brien, J. Wittes, R. Wirtz, J. Cohen, W. R. Ballou; RTS,S Malaria Vaccine Evaluation, A phase I/IIa safety, immunogenicity, and efficacy bridging randomized study of a two-dose regimen of liquid and lyophilized formulations of the candidate malaria vaccine RTS,S/AS02A in malaria-naive adults. *Vaccine* **25**, 5359–5366 (2007).
18. P. Sun, R. Schwenk, K. White, J. A. Stoute, J. Cohen, W. R. Ballou, G. Voss, K. E. Kester, D. G. Heppner, U. Krzych, Protective immunity induced with malaria vaccine, RTS,S, is linked to *Plasmodium falciparum* circumsporozoite protein-specific $CD4^+$ and $CD8^+$ T cells producing IFN-γ. *J. Immunol.* **171**, 6961–6967 (2003).
19. S. Chaudhury, C. F. Ockenhouse, J. A. Regules, S. Dutta, A. Wallqvist, E. Jongert, N. C. Waters, F. Lemiale, E. Bergmann-Leitner, The biological function of antibodies

induced by the RTS,S/AS01 malaria vaccine candidate is determined by their fine specificity. *Malar. J.* **15**, 301 (2016).
20. D. Kazmin, H. I. Nakaya, E. K. Lee, M. J. Johnson, R. van der Most, R. A. van den Berg, W. R. Ballou, E. Jongert, U. Wille-Reece, C. Ockenhouse, A. Aderem, D. E. Zak, J. Sadoff, J. Hendriks, J. Wrammert, R. Ahmed, B. Pulendran, Systems analysis of protective immune responses to RTS,S malaria vaccination in humans. *Proc. Natl. Acad. Sci. U.S.A.* **114**, 2425–2430 (2017).
21. R. A. van den Berg, M. Coccia, W. R. Ballou, K. E. Kester, C. F. Ockenhouse, J. Vekemans, E. Jongert, A. M. Didierlaurent, R. G. van der Most, Predicting RTS,S vaccine-mediated protection from transcriptomes in a malaria-challenge clinical trial. *Front. Immunol.* **8**, 557 (2017).
22. M. T. Vahey, Z. Wang, K. E. Kester, J. Cummings, D. G. Heppner Jr., M. E. Nau, O. Ofori-Anyinam, J. Cohen, T. Coche, W. R. Ballou, C. F. Ockenhouse, Expression of genes associated with immunoproteasome processing of major histocompatibility complex peptides is indicative of protection with adjuvanted RTS,S malaria vaccine. *J. Infect. Dis.* **201**, 580–589 (2010).
23. A. Horowitz, J. C. Hafalla, E. King, J. Lusingu, D. Dekker, A. Leach, P. Moris, J. Cohen, J. Vekemans, T. Villafana, P. H. Corran, P. Bejon, C. J. Drakeley, L. von Seidlein, E. M. Riley, Antigen-specific IL-2 secretion correlates with NK cell responses after immunization of Tanzanian children with the RTS,S/AS01 malaria vaccine. *J. Immunol.* **188**, 5054–5062 (2012).
24. P. Moris, E. Jongert, R. G. van der Most, Characterization of T-cell immune responses in clinical trials of the candidate RTS,S malaria vaccine. *Hum. Vaccin. Immunother.* **14**, 17–27 (2018).
25. M. T. White, R. Verity, J. T. Griffin, K. P. Asante, S. Owusu-Agyei, B. Greenwood, C. Drakeley, S. Gesase, J. Lusingu, D. Ansong, S. Adjei, T. Agbenyega, B. Ogutu, L. Otieno, W. Otieno, S. T. Agnandji, B. Lell, P. Kremsner, I. Hoffman, F. Martinson, P. Kamthunzu, H. Tinto, I. Valea, H. Sorgho, M. Oneko, K. Otieno, M. J. Hamel, N. Salim, A. Mtoro, S. Abdulla, P. Aide, J. Sacarlal, J. J. Aponte, P. Njuguna, K. Marsh, P. Bejon, E. M. Riley, A. C. Ghani, Immunogenicity of the RTS,S/AS01 malaria vaccine and implications for duration of vaccine efficacy: Secondary analysis of data from a phase 3 randomised controlled trial. *Lancet. Infectious diseases* **15**, 1450–1458 (2015).
26. M. T. White, P. Bejon, A. Olotu, J. T. Griffin, K. Bojang, J. Lusingu, N. Salim, S. Abdulla, N. Otsyula, S. T. Agnandji, B. Lell, K. P. Asante, S. Owusu-Agyei, E. Mahama, T. Agbenyega, D. Ansong, J. Sacarlal, J. J. Aponte, A. C. Ghani, A combined analysis of immunogenicity, antibody kinetics and vaccine efficacy from phase 2 trials of the RTS,S malaria vaccine. *BMC Med.* **12**, 117 (2014).
27. S. A. Plotkin, Correlates of protection induced by vaccination. *Clin. Vaccine Immunol.* **17**, 1055–1065 (2010).
28. S. Bournazos, J. V. Ravetch, Fcγ receptor function and the design of vaccination strategies. *Immunity* **47**, 224–233 (2017).
29. L. L. Lu, T. J. Suscovich, S. M. Fortune, G. Alter, Beyond binding: Antibody effector functions in infectious diseases. *Nat. Rev. Immunol.* **18**, 46–61 (2018).
30. H. A. Vanderven, S. J. Kent, The protective potential of Fc-mediated antibody functions against influenza virus and other viral pathogens. *Immunol. Cell Biol.* **98**, 253–263 (2020).
31. J. T. Earnest, K. Basore, V. Roy, A. L. Bailey, D. Wang, G. Alter, D. H. Fremont, M. S. Diamond, Neutralizing antibodies against Mayaro virus require Fc effector functions for protective activity. *J. Exp. Med.* **216**, 2282–2301 (2019).
32. E. A. van Erp, W. Luytjes, G. Ferwerda, P. B. van Kasteren, Fc-mediated antibody effector functions during respiratory syncytial virus infection and disease. *Front. Immunol.* **10**, 548 (2019).
33. B. M. Gunn, W. H. Yu, M. M. Karim, J. M. Brannan, A. S. Herbert, A. Z. Wec, P. J. Halfmann, M. L. Fusco, S. L. Schendel, K. Gangavarapu, T. Krause, X. Qiu, S. He, J. Das, T. J. Suscovich, J. Lai, K. Chandran, L. Zeitlin, J. E. Crowe Jr., D. Lauffenburger, Y. Kawaoka, G. P. Kobinger, K. G. Andersen, J. M. Dye, E. O. Saphire, G. Alter, A role for Fc function in therapeutic monoclonal antibody-mediated protection against ebola virus. *Cell Host Microbe* **24**, 221–233.e5 (2018).
34. D. J. DiLillo, P. Palese, P. C. Wilson, J. V. Ravetch, Broadly neutralizing anti-influenza antibodies require Fc receptor engagement for in vivo protection. *J. Clin. Invest.* **126**, 605–610 (2016).
35. A. W. Chung, M. P. Kumar, K. B. Arnold, W. H. Yu, M. K. Schoen, L. J. Dunphy, T. J. Suscovich, N. Frahm, C. Linde, A. E. Mahan, M. Hoffner, H. Streeck, M. E. Ackerman, M. J. McElrath, H. Schuitemaker, M. G. Pau, L. R. Baden, J. H. Kim, N. L. Michael, D. H. Barouch, D. A. Lauffenburger, G. Alter, Dissecting polyclonal vaccine-induced humoral immunity against HIV using systems serology. *Cell* **163**, 988–998 (2015).
36. T. Hastie, R. Tibshirani, J. H. Friedman, *The Elements of Statistical Learning : Data Mining, Inference, and Prediction*, Springer series in statistics, (Springer, ed. 2, 2009), pp. xxii, pp. 745.
37. E. Aliprandini, J. Tavares, R. H. Panatieri, S. Thiberge, M. M. Yamamoto, O. Silvie, T. Ishino, M. Yuda, S. Dartevelle, F. Traincard, S. B. Boscardin, R. Amino, Cytotoxic anti-circumsporozoite antibodies target malaria sporozoites in the host skin. *Nat. Microbiol.* **3**, 1224–1233 (2018).
38. N. K. Kisalu, A. H. Idris, C. Weidle, Y. Flores-Garcia, B. J. Flynn, B. K. Sack, S. Murphy, A. Schon, E. Freire, J. R. Francica, A. B. Miller, J. Gregory, S. March, H. X. Liao, B. F. Haynes, K. Wiehe, A. M. Trama, K. O. Saunders, M. A. Gladden, A. Monroe, M. Bonsignori, M. Kanekiyo, A. K. Wheatley, A. B. McDermott, S. K. Farney, G. Y. Chuang, B. Zhang, N. Kc, S. Chakravarty, P. D. Kwong, P. Sinnis, S. N. Bhatia, S. H. I. Kappe, B. K. L. Sim, S. L. Hoffman, F. Zavala, M. Pancera, R. A. Seder, A human monoclonal antibody prevents malaria infection by targeting a new site of vulnerability on the parasite. *Nat. Med.* **24**, 408–416 (2018).
39. B. K. Sack, S. A. Mikolajczak, M. Fishbaugher, A. M. Vaughan, E. L. Flannery, T. Nguyen, W. Betz, M. Jane Navarro, L. Foquet, R. W. J. Steel, Z. P. Billman, S. C. Murphy, S. L. Hoffman, S. Chakravarty, B. K. L. Sim, M. Behet, I. J. Reuling, J. Walk, A. Scholzen, R. W. Sauerwein, A. S. Ishizuka, B. Flynn, R. A. Seder, S. H. I. Kappe, Humoral protection against mosquito bite-transmitted *Plasmodium falciparum* infection in humanized mice. *NPJ Vaccines* **2**, 27 (2017).
40. Y. Flores-Garcia, G. Nasir, C. S. Hopp, C. Munoz, A. E. Balaban, F. Zavala, P. Sinnis, Antibody-mediated protection against *Plasmodium sporozoites* begins at the dermal inoculation site. *mBio* **9**, e02194-18 (2018).
41. R. W. Steel, B. K. Sack, M. Tsuji, M. J. Navarro, W. Betz, M. E. Fishbaugher, E. L. Flannery, S. H. Kappe, An opsonic phagocytosis assay for *Plasmodium falciparum* sporozoites. *Clin. Vaccine Immunol.* **24**, –e00445-16 (2017).
42. D. Oyen, J. L. Torres, U. Wille-Reece, C. F. Ockenhouse, D. Emerling, J. Glanville, W. Volkmuth, Y. Flores-Garcia, F. Zavala, A. B. Ward, C. R. King, I. A. Wilson, Structural basis for antibody recognition of the NANP repeats in *Plasmodium falciparum* circumsporozoite protein. *Proc. Natl. Acad. Sci. U.S.A.* **114**, E10438–E10445 (2017).
43. S. March, V. Ramanan, K. Trehan, S. Ng, A. Galstian, N. Gural, M. A. Scull, A. Shlomai, M. M. Mota, H. E. Fleming, S. R. Khetani, C. M. Rice, S. N. Bhatia, Micropatterned coculture of primary human hepatocytes and supportive cells for the study of hepatotropic pathogens. *Nat. Protoc.* **10**, 2027–2053 (2015).
44. A. Barry, M. C. Behet, I. Nebie, K. Lanke, L. Grignard, A. Ouedraogo, I. Soulama, C. Drakeley, R. Sauerwein, J. M. Bolscher, K. J. Dechering, T. Bousema, A. B. Tiono, B. P. Goncalves, Functional antibodies against *Plasmodium falciparum* sporozoites are associated with a longer time to qPCR-detected infection among schoolchildren in Burkina Faso. *Wellcome Open Res.* **3**, 159 (2018).
45. G. Arora, G. T. Hart, J. Manzella-Lapeira, J. Y. Doritchamou, D. L. Narum, L. M. Thomas, J. Brzostowski, S. Rajagopalan, O. K. Doumbo, B. Traore, L. H. Miller, S. K. Pierce, P. E. Duffy, P. D. Crompton, S. A. Desai, E. O. Long, NK cells inhibit *Plasmodium falciparum* growth in red blood cells via antibody-dependent cellular cytotoxicity. *eLife* **7**, e36806 (2018).
46. L. Mac-Daniel, M. R. Buckwalter, M. Berthet, Y. Virk, K. Yui, M. L. Albert, P. Gueirard, R. Menard, Local immune response to injection of Plasmodium sporozoites into the skin. *J. Immunol.* **193**, 1246–1257 (2014).
47. L. Kurtovic, M. J. Boyle, D. H. Opi, A. T. Kennedy, W. H. Tham, L. Reiling, J. A. Chan, J. G. Beeson, Complement in malaria immunity and vaccines. *Immunol. Rev.* **293**, 38–56 (2020).
48. E. H. Aitken, A. Alemu, S. J. Rogerson, Neutrophils and malaria. *Front. Immunol.* **9**, 3005 (2018).
49. F. H. Osier, G. Feng, M. J. Boyle, C. Langer, J. Zhou, J. S. Richards, F. J. McCallum, L. Reiling, A. Jaworowski, R. F. Anders, K. Marsh, J. G. Beeson, Opsonic phagocytosis of Plasmodium falciparum merozoites: Mechanism in human immunity and a correlate of protection against malaria. *BMC Med.* **12**, 108 (2014).
50. S. Sidjanski, J. P. Vanderberg, Delayed migration of *Plasmodium* sporozoites from the mosquito bite site to the blood. *Am. J. Trop. Med. Hyg.* **57**, 426–429 (1997).
51. S. C. Shin, J. P. Vanderberg, J. A. Terzakis, Direct infection of hepatocytes by sporozoites of Plasmodium berghei. *J. Protozool.* **29**, 448–454 (1982).
52. B. Clemenceau, R. Vivien, M. Berthome, N. Robillard, R. Garand, G. Gallot, S. Vollant, H. Vie, Effector memory αβ T lymphocytes can express FcγRIIIa and mediate antibody-dependent cellular cytotoxicity. *J. Immunol.* **180**, 5327–5334 (2008).
53. J. Brozova, I. Karlova, J. Novak, Analysis of the phenotype and function of the subpopulations of mucosal-associated invariant T cells. *Scand. J. Immunol.* **84**, 245–251 (2016).
54. X. Fan, L. Zhu, H. Liang, Z. Xie, X. Huang, S. Wang, T. Shen, Antibody-dependent CD56+ T cell responses are functionally impaired in long-term HIV-1 infection. *Retrovirology* **13**, 76 (2016).
55. K. S. Burrack, G. T. Hart, S. E. Hamilton, Contributions of natural killer cells to the immune response against Plasmodium. *Malar. J.* **18**, 321 (2019).
56. J. Mikulak, E. Bruni, F. Oriolo, C. Di Vito, D. Mavilio, Hepatic natural killer cells: Organ-specific sentinels of liver immune homeostasis and physiopathology. *Front. Immunol.* **10**, 946 (2019).
57. J. P. Gigley, The diverse role of NK cells in immunity to toxoplasma gondii infection. *PLOS Pathog.* **12**, e1005396 (2016).
58. S. M. Dann, H. C. Wang, K. J. Gambarin, J. K. Actor, P. Robinson, D. E. Lewis, S. Caillat-Zucman, A. C. White Jr., Interleukin-15 activates human natural killer cells to clear the intestinal protozoan cryptosporidium. *J Infect Dis* **192**, 1294–1302 (2005).

59. C. Bogdan, Natural killer cells in experimental and human leishmaniasis. *Front. Cell. Infect. Microbiol.* **2**, 69 (2012).
60. D. E. Neafsey, M. Juraska, T. Bedford, D. Benkeser, C. Valim, A. Griggs, M. Lievens, S. Abdulla, S. Adjei, T. Agbenyega, S. T. Agnandji, P. Aide, S. Anderson, D. Ansong, J. J. Aponte, K. P. Asante, P. Bejon, A. J. Birkett, M. Bruls, K. M. Connolly, U. D'Alessandro, C. Dobano, S. Gesase, B. Greenwood, J. Grimsby, H. Tinto, M. J. Hamel, I. Hoffman, P. Kamthunzi, S. Kariuki, P. G. Kremsner, A. Leach, B. Lell, N. J. Lennon, J. Lusingu, K. Marsh, F. Martinson, J. T. Molel, E. L. Moss, P. Njuguna, C. F. Ockenhouse, B. R. Ogutu, W. Otieno, L. Otieno, K. Otieno, S. Owusu-Agyei, D. J. Park, K. Pelle, D. Robbins, C. Russ, E. M. Ryan, J. Sacarlal, B. Sogoloff, H. Sorgho, M. Tanner, T. Theander, I. Valea, S. K. Volkman, Q. Yu, D. Lapierre, B. W. Birren, P. B. Gilbert, D. F. Wirth, Genetic diversity and protective efficacy of the RTS,S/AS01 malaria vaccine. *N. Engl. J. Med.* **373**, 2025–2037 (2015).
61. C. Dobaño, H. Sanz, H. Sorgho, D. Dosoo, M. Mpina, I. Ubillos, R. Aguilar, T. Ford, N. Díez-Padrisa, N. A. Williams, A. Ayestaran, O. Traore, A. J. Nhabomba, C. Jairoce, J. Waitumbi, S. T. Agnandji, S. Kariuki, S. Abdulla, J. J. Aponte, B. Mordmüller, K. P. Asante, S. Owusu-Agyei, H. Tinto, J. J. Campo, G. Moncunill, B. Gyan, C. Valim, C. Daubenberger, Concentration and avidity of antibodies to different circumsporozoite epitopes correlate with RTS,S/AS01E malaria vaccine efficacy. *Nat. Commun.* **10**, 2174 (2019).
62. I. Ubillos, A. Ayestaran, A. J. Nhabomba, D. Dosoo, M. Vidal, A. Jiménez, C. Jairoce, H. Sanz, R. Aguilar, N. A. Williams, N. Díez-Padrisa, M. Mpina, H. Sorgho, S. T. Agnandji, S. Kariuki, B. Mordmüller, C. Daubenberger, K. P. Asante, S. Owusu-Agyei, J. Sacarlal, P. Aide, J. J. Aponte, S. Dutta, B. Gyan, J. J. Campo, C. Valim, G. Moncunill, C. Dobaño, Baseline exposure, antibody subclass, and hepatitis B response differentially affect malaria protective immunity following RTS,S/AS01E vaccination in African children. *BMC Med.* **16**, 197 (2018).
63. C. Dobaño, R. Santano, M. Vidal, A. Jiménez, C. Jairoce, I. Ubillos, D. Dosoo, R. Aguilar, N. A. Williams, N. Díez-Padrisa, A. Ayestaran, C. Valim, K. P. Asante, S. Owusu-Agyei, D. Lanar, V. Chauhan, C. Chitnis, S. Dutta, E. Angov, B. Gamain, R. L. Coppel, J. G. Beeson, L. Reiling, D. Gaur, D. Cavanagh, B. Gyan, A. J. Nhabomba, J. J. Campo, G. Moncunill, Differential patterns of IgG subclass responses to *Plasmodium falciparum* antigens in relation to malaria protection and RTS,S vaccination. *Front. Immunol.* **10**, 439 (2019).
64. D. L. Hill, E. J. Carr, T. Rutishauser, G. Moncunill, J. J. Campo, S. Innocentin, M. Mpina, A. Nhabomba, A. Tumbo, C. Jairoce, H. A. Moll, M. C. van Zelm, C. Dobaño, C. Daubenberger, M. A. Linterman, Immune system development varies according to age, location, and anemia in African children. *Sci. Transl. Med.* **12**, eaaw9522 (2020).
65. M. F. Jennewein, I. Goldfarb, S. Dolatshahi, C. Cosgrove, F. J. Noelette, M. Krykbaeva, J. Das, A. Sarkar, M. J. Gorman, S. Fischinger, C. M. Boudreau, J. Brown, J. H. Cooperrider, J. Aneja, T. J. Suscovich, B. S. Graham, G. M. Lauer, T. Goetghebuer, A. Marchant, D. Lauffenburger, A. Y. Kim, L. E. Riley, G. Alter, Fc glycan-mediated regulation of placental antibody transfer. *Cell* **178**, 202–215.e14 (2019).
66. S. M. Lawrence, R. Corriden, V. Nizet, Age-appropriate functions and dysfunctions of the neonatal neutrophil. *Front. Pediatr.* **5**, 23 (2017).
67. K. E. Schuit, D. A. Powell, Phagocytic dysfunction in monocytes of normal newborn infants. *Pediatrics* **65**, 501–504 (1980).
68. J. R. Francica, D. E. Zak, C. Linde, E. Siena, C. Johnson, M. Juraska, N. L. Yates, B. Gunn, E. De Gregorio, B. J. Flynn, N. M. Valiante, P. Malyala, S. W. Barnett, P. Sarkar, M. Singh, S. Jain, M. Ackerman, M. Alam, G. Ferrari, A. Salazar, G. D. Tomaras, D. T. O'Hagan, A. Aderem, G. Alter, R. A. Seder, Innate transcriptional effects by adjuvants on the magnitude, quality, and durability of HIV envelope responses in NHPs. *Blood Adv.* **1**, 2329–2342 (2017).
69. M. Spring, M. Polhemus, C. Ockenhouse, Controlled human malaria infection. *J. Infect. Dis.* **209** Suppl 2, S40–S45 (2014).
70. R. Schwenk, M. DeBot, M. Porter, J. Nikki, L. Rein, R. Spaccapelo, A. Crisanti, P. D. Wightman, C. F. Ockenhouse, S. Dutta, IgG2 antibodies against a clinical grade *Plasmodium falciparum* CSP vaccine antigen associate with protection against transgenic sporozoite challenge in mice. *PLOS ONE* **9**, e111020 (2014).
71. G. Folena-Wasserman, R. Inacker, J. Rosenbloom, Assay, purification and characterization of a recombinant malaria circumsporozoite fusion protein by high-performance liquid chromatography. *J. Chromatogr.* **411**, 345–354 (1987).
72. H. K. Lyerly, D. L. Reed, T. J. Matthews, A. J. Langlois, P. A. Ahearne, S. R. Petteway Jr., K. J. Weinhold, Anti-GP 120 antibodies from HIV seropositive individuals mediate broadly reactive anti-HIV ADCC. *AIDS Res. Hum. Retroviruses* **3**, 409–422 (1987).
73. D. N. Howell, P. E. Andreotti, J. R. Dawson, P. Cresswell, Natural killing target antigens as inducers of interferon: Studies with an immunoselected, natural killing-resistant human T lymphoblastoid cell line. *J. Immunol.* **134**, 971–976 (1985).
74. M. E. Ackerman, B. Moldt, R. T. Wyatt, A.-S. Dugast, E. McAndrew, S. Tsoukas, S. Jost, C. T. Berger, G. Sciaranghella, Q. Liu, D. J. Irvine, D. R. Burton, G. Alter, A robust, high-throughput assay to determine the phagocytic activity of clinical antibody samples. *J. Immunol. Methods* **366**, 8–19 (2011).
75. S. Fischinger, J. K. Fallon, A. R. Michell, T. Broge, T. J. Suscovich, H. Streeck, G. Alter, A high-throughput, bead-based, antigen-specific assay to assess the ability of antibodies to induce complement activation. *J. Immunol. Methods* **473**, 112630 (2019).
76. S. Jegaskanda, E. R. Job, M. Kramski, K. Laurie, G. Isitman, R. de Rose, W. R. Winnall, I. Stratov, A. G. Brooks, P. C. Reading, S. J. Kent, Cross-reactive influenza-specific antibody-dependent cellular cytotoxicity antibodies in the absence of neutralizing antibodies. *J. Immunol.* **190**, 1837–1848 (2013).
77. L. L. Lu, A. W. Chung, T. R. Rosebrock, M. Ghebremichael, W. H. Yu, P. S. Grace, M. K. Schoen, F. Tafesse, C. Martin, V. Leung, A. E. Mahan, M. Sips, M. P. Kumar, J. Tedesco, H. Robinson, E. Tkachenko, M. Draghi, K. J. Freedberg, H. Streeck, T. J. Suscovich, D. A. Lauffenburger, B. I. Restrepo, C. Day, S. M. Fortune, G. Alter, A functional role for antibodies in tuberculosis. *Cell* **167**, 433–443.e14 (2016).
78. V. R. Gómez-Román, R. H. Florese, L. J. Patterson, B. Peng, D. Venzon, K. Aldrich, M. Robert-Guroff, A simplified method for the rapid fluorometric assessment of antibody-dependent cell-mediated cytotoxicity. *J. Immunol. Methods* **308**, 53–67 (2006).
79. E. P. Brown, A. F. Licht, A. S. Dugast, I. Choi, C. Bailey-Kellogg, G. Alter, M. E. Ackerman, High-throughput, multiplexed IgG subclassing of antigen-specific antibodies from clinical samples. *J. Immunol. Methods* **386**, 117–123 (2012).
80. E. P. Brown, K. G. Dowell, A. W. Boesch, E. Normandin, A. E. Mahan, T. Chu, D. H. Barouch, C. Bailey-Kellogg, G. Alter, M. E. Ackerman, Multiplexed Fc array for evaluation of antigen-specific antibody effector profiles. *J. Immunol. Methods* **443**, 33–44 (2017).
81. E. P. Brown, J. A. Weiner, S. Lin, H. Natarajan, E. Normandin, D. H. Barouch, G. Alter, M. Sarzotti-Kelsoe, M. E. Ackerman, Optimization and qualification of an Fc Array assay for assessments of antibodies against HIV-1/SIV. *J. Immunol. Methods* **455**, 24–33 (2018).
82. A. E. Mahan, J. Tedesco, K. Dionne, K. Baruah, H. D. Cheng, P. L. De Jager, D. H. Barouch, T. Suscovich, M. Ackerman, M. Crispin, G. Alter, A method for high-throughput, sensitive analysis of IgG Fc and Fab glycosylation by capillary electrophoresis. *J. Immunol. Methods* **417**, 34–44 (2015).
83. E. P. Brown, E. Normandin, N. Y. Osei-Owusu, A. E. Mahan, Y. N. Chan, J. I. Lai, M. Vaccari, M. Rao, G. Franchini, G. Alter, M. E. Ackerman, Microscale purification of antigen-specific antibodies. *J. Immunol. Methods* **425**, 27–36 (2015).
84. M. E. Smoot, K. Ono, J. Ruscheinski, P.-L. Wang, T. Ideker, Cytoscape 2.8: New features for data integration and network visualization. *Bioinformatics* **27**, 431–432 (2011).
85. M. E. Ackerman, J. Das, S. Pittala, T. Broge, C. Linde, T. J. Suscovich, E. P. Brown, T. Bradley, H. Natarajan, S. Lin, J. K. Sassic, S. O'Keefe, N. Mehta, D. Goodman, M. Sips, J. A. Weiner, G. D. Tomaras, B. F. Haynes, D. A. Lauffenburger, C. Bailey-Kellogg, M. Roederer, G. Alter, Route of immunization defines multiple mechanisms of vaccine-mediated protection against SIV. *Nat. Med.* **24**, 1590–1598 (2018).
86. R. Tibshirani, Regression shrinkage and selection via the lasso. *J. R. Stat. Soc. B Met.* **58**, 267–288 (1996).
87. C. Cortes, V. Vapnik, Support-vector networks. *Mach. Learn.* **20**, 273–297 (1995).
88. M. Ojala, G. C. Garriga, Permutation tests for studying classifier performance. *J. Mach. Learn. Res.* **11**, 1833–1863 (2010).
89. J. E. Epstein, K. Tewari, K. E. Lyke, B. K. L. Sim, P. F. Billingsley, M. B. Laurens, A. Gunasekera, S. Chakravarty, E. R. James, M. Sedegah, A. Richman, S. Velmurugan, S. Reyes, M. Li, K. Tucker, A. Ahumada, A. J. Ruben, T. Li, R. Stafford, A. G. Eappen, C. Tamminga, J. W. Bennett, C. F. Ockenhouse, J. R. Murphy, J. Komisar, N. Thomas, M. Loyevsky, A. Birkett, C. V. Plowe, C. Loucq, R. Edelman, T. L. Richie, R. A. Seder, S. L. Hoffman, J. E. Epstein, K. Tewari, K. E. Lyke, B. K. L. Sim, P. F. Billingsley, M. B. Laurens, A. Gunasekera, S. Chakravarty, E. R. James, M. Sedegah, A. Richman, S. Velmurugan, S. Reyes, M. Li, K. Tucker, A. Ahumada, A. J. Ruben, T. Li, R. Stafford, A. G. Eappen, C. Tamminga, J. W. Bennett, C. F. Ockenhouse, J. R. Murphy, J. Komisar, N. Thomas, M. Loyevsky, A. Birkett, C. V. Plowe, C. Loucq, R. Edelman, T. L. Richie, R. A. Seder, S. L. Hoffman, Live attenuated malaria vaccine designed to protect through hepatic $CD8^+$ T cell immunity. *Science* **334**, 475–480 (2011).
90. S. L. Hoffman, P. F. Billingsley, E. James, A. Richman, M. Loyevsky, T. Li, S. Chakravarty, A. Gunasekera, R. Chattopadhyay, M. Li, R. Stafford, A. Ahumada, J. E. Epstein, M. Sedegah, S. Reyes, T. L. Richie, K. E. Lyke, R. Edelman, M. B. Laurens, C. V. Plowe, B. K. L. Sim, Development of a metabolically active, non-replicating sporozoite vaccine to prevent *Plasmodium falciparum* malaria. *Hum. Vaccin.* **6**, 97–106 (2010).
91. Y. Flores-Garcia, S. M. Herrera, H. Jhun, D. W. Pérez-Ramos, C. R. King, E. Locke, R. Raghunandan, F. Zavala, Optimization of an in vivo model to study immunity to *Plasmodium falciparum* pre-erythrocytic stages. *Malar. J.* **18**, 426 (2019).

Acknowledgments: We thank the participants of the studies. All clinical studies were performed at the Walter Reed Army Institute of Research, Malaria Vaccine Branch, and serum samples were provided by GSK. We thank the insectary and parasitology core facilities at the Johns Hopkins Bloomberg School of Public Health and Harvard School of Public Health for providing *P. falciparum*–infected mosquitoes. The Johns Hopkins Bloomberg School of Public Health Insectary is supported by Bloomberg Philanthropies. We also thank the Swanson Biotechnology Center at the Koch Institute for Integrative Cancer Research at MIT and specifically D. Mankus, M. Bisher, and A. Lytton-Jean in the Nanotechnology Materials Core for assistance with SEM imaging. Last, we thank A. Birkett, R. King, L. Schuerman, R. Van Der Most, B. Salaun, and M. Lievens for review of the manuscript. **Funding:** This research was supported by PATH's Malaria Vaccine Initiative (GAT.0888-30-01617579-COL to G.A.), the

MGH Research Scholars program, and the Ragon Institute of MGH, MIT, and Harvard. SNB is an HHMI investigator. **Author contributions:** Conceptualization: T.J.S., E.J., U.W.-R., and G.A. Data curation: J.D. Formal analysis: J.D. Funding acquisition: G.A. Investigation: J.K.F., A.R.D., J.C., C.H.L., A.M., H.N., C.A., T.B., T.L., V.K., R.L., M.D.S., M.M., S.M., J.W., and Y.F.-G. Methodology: T.J.S., D.A.L., and G.A. Project administration: T.J.S., C.L., S.G., and G.A. Resources: F.Z., S.D., J.H., E.J., and G.A. Software: J.D. Supervision: T.J.S., C.L., S.G., F.Z., M.E.A., S.N.B., D.A.L., and G.A. Validation: T.J.S., J.K.F., J.D., A.R.D., and G.A. Visualization: T.J.S. and G.A. Writing (original draft): T.J.S. and G.A. Writing (review and editing): T.J.S., J.K.F., J.D., A.R.D., J.C., V.K., C.H.L., M.C., M.E.A., E.B.-L., J.H., J.S., S.D., D.A.L., E.J., U.W.-R., and G.A. **Competing interests:** E.J. and M.C. are employees of GSK group of companies. J.H. and J.S. are employees of Janssen, Pharmaceutical Companies of Johnson & Johnson. E.J. and M.C. report ownership of shares and/or restricted shares of the GSK group of companies. S.N.B. and G.A. have received sponsored research funds from Johnson & Johnson and Janssen Pharmaceuticals. T.J.S., C.H.L., C.L., T.L., T.B., and G.A. own shares in SeromYx Systems, Inc. G.A. is an inventor on patent application WO2017184733A1 submitted by Massachusetts General Hospital that covers Systems Serology. M.C. is an inventor on patent WO2018114892A1 held by GSK that covers methods for adjuvanting the immune response to an antigen via the separate administration of a saponin and a TLR4 agonist. The other authors declare no competing interests. **Data and materials availability:** All data associated with this study are present in the paper or the Supplementary Materials.

Submitted 26 February 2020
Accepted 2 June 2020
Published 22 July 2020
10.1126/scitranslmed.abb4757

Citation: T. J. Suscovich, J. K. Fallon, J. Das, A. R. Demas, J. Crain, C. H. Linde, A. Michell, H. Natarajan, C. Arevalo, T. Broge, T. Linnekin, V. Kulkarni, R. Lu, M. D. Slein, C. Luedemann, M. Marquette, S. March, J. Weiner, S. Gregory, M. Coccia, Y. Flores-Garcia, F. Zavala, M. E. Ackerman, E. Bergmann-Leitner, J. Hendriks, J. Sadoff, S. Dutta, S. N. Bhatia, D. A. Lauffenburger, E. Jongert, U. Wille-Reece, G. Alter, Mapping functional humoral correlates of protection against malaria challenge following RTS,S/AS01 vaccination. *Sci. Transl. Med.* **12**, eabb4757 (2020).

Science Translational Medicine

Mapping functional humoral correlates of protection against malaria challenge following RTS,S/AS01 vaccination

Todd J. Suscovich, Jonathan K. Fallon, Jishnu Das, Allison R. Demas, Jonathan Crain, Caitlyn H. Linde, Ashlin Michell, Harini Natarajan, Claudia Arevalo, Thomas Broge, Thomas Linnekin, Viraj Kulkarni, Richard Lu, Matthew D. Slein, Corinne Luedemann, Meghan Marquette, Sandra March, Joshua Weiner, Scott Gregory, Margherita Coccia, Yevel Flores-Garcia, Fidel Zavala, Margaret E. Ackerman, Elke Bergmann-Leitner, Jenny Hendriks, Jerald Sadoff, Sheetij Dutta, Sangeeta N. Bhatia, Douglas A. Lauffenburger, Erik Jongert, Ulrike Wille-Reece and Galit Alter

Sci Transl Med **12**, eabb4757.
DOI: 10.1126/scitranslmed.abb4757

Above and beyond antibody abundance

Vaccine development can be hampered by a lack of clear correlates of protection. Suscovich *et al.* applied systems serology to samples from studies with the RTS,S/AS01 vaccine to understand which antibody functions were associated with protection from controlled malaria challenge, as magnitude of antibody response alone was not predictive. Systems serology revealed that a very small number of parameters involving engagement of innate immune cells could predict protection; this was confirmed with data from two additional studies. Experiments with antibodies in vitro or administered to mice further demonstrated the importance of Fc-mediated functions and innate immunity for protection from malaria parasites. This study emphasizes that finding correlates of protection requires investigation beyond measuring antibody abundance.